Thesis for the degree of Licenciate of Engineering

Microwave Gaussian quantum metrology

Robert S. Jonsson

Department of Microtechnology and Nanoscience (MC2)
Applied Quantum Physics Laboratory
Chalmers University of Technology
Göteborg, Sweden 2023

Microwave Gaussian quantum metrology
Robert S. Jonsson

Thesis for the degree of Licenciate of Engineering
ISSN 1652–0769
Technical Report no. MC2–463

Chalmers University of Technology
Department of Microtechnology and Nanoscience – MC2
Applied Quantum Physics Laboratory
SE-412 96 Göteborg, Sweden
Phone: +46 (0)31–772 1000

Printed by Chalmers Digitaltryck
Göteborg, Sweden 2023

Microwave Gaussian quantum metrology

ROBERT S. JONSSON

Applied Quantum Physics Laboratory
Department of Microtechnology and Nanoscience – MC2
Chalmers University of Technology

Abstract

With increasingly sensitive measurements being made possible by technological development, there arises situations where the effects of quantum mechanics have to be taken into account. While quantum mechanics tells us that there are fundamental limits of measurement sensitivity, it also gives us the tools to constructively push the same limits for experimental systems. The field of quantum metrology investigates how sensitive a measurement can be made, and how to realize such a setup.

Quantum metrology as a topic is well established for the field of quantum optics in the visible light frequency range, and quantum enhanced measurement setups have been experimentally realized. In the last couple of decades, similar types of setups are starting to be possible at microwave frequencies, where a thermal background can be significant.

In this thesis and the appended articles, we have studied various quantum probes applied to radar-like scenarios where the task is to measure a weak signal in the presence of thermal noise. Our focus has been two-fold. On the one hand, we have studied the quantum illumination protocol which uses entanglement to beat classical protocols in the task of binary discrimination. We have elucidated the scenario where an advantage is realized and argued that it is difficult to find useful applications for the protocol. On the other hand, we have studied the task of estimating the attenuation coefficient in a lossy Bosonic channel, and established the optimal Gaussian probe states based on maximization of quantum Fisher information. These results serve to illustrate situations where a proper understanding of quantum mechanics can be applied to enhance radar-like tasks, or quantum radars.

Keywords: Quantum Radar, Quantum Sensing, Gaussian, Quantum Fisher Information, Bosonic channel

List of publications

Appended publications

[I] **R. Jonsson**, R. Di Candia, M. Ankel, A. Ström, G. Johansson, "A comparison between quantum and classical noise radar sources", *2020 IEEE Radar Conference (RadarConf2020)*, pp. 1 – 6, 2020.
DOI: `10.1109/RadarConf2043947.2020.9266597`

[II] **R. Jonsson**, M. Ankel, "Quantum Radar – What is it good for?", *2021 IEEE Radar Conference (RadarConf2021)*, pp. 1 – 6, 2021.
DOI: `10.1109/RadarConf2147009.2021.9455162`

[III] **R. Jonsson**, R. Di Candia, "Gaussian quantum estimation of the loss parameter in a thermal environment", *J. Phys. A: Math. Theor.*, vol. 55, no. 385301, 2022.
DOI: `10.1088/1751-8121/ac83fa`

Other publications

[A] M. Ankel, **R. Jonsson**, T. Bryllert, L.M.H. Ulander, P. Delsing, "Bistatic noise radar: Demonstration of correlation noise suppression", *IET Radar, Sonar & Navig.*, vol. 17, no. 3, pp. 351 – 361, 2023.
DOI: `10.1049/rsn2.12345`

[B] D. Fitzek, **R.S. Jonsson**, W. Dobrautz, C. Schäfer, "Optimizing Variational Quantum Algorithms with qBang: Efficiently Interweaving Metric and Momentum to Tackle Flat Energy Landscapes", *arXiv:2304.13882* ***[quant-ph]***, 2023.
DOI: `10.48550/arXiv.2304.13882`

Acknowledgement

There are many people that have been involved in making this thesis possible. I am grateful for the many helpful discussions I have had with my supervisor Göran Johansson. Similarly, my industrial supervisor Anders Ström has contributed with many excellent insights and suggestions. The research work that lead to the publications covered in this thesis have been made in close collaboration with Roberto Di Candia and Martin Ankel. Finally, I consider myself lucky to be part of not one but two fantastic groups: Applied Quantum Physics at Chalmers, and Research and Concepts at Saab. Going to work in an office with such clever people is always a pleasure!

Contents

Abstract i

List of publications iii

Acknowledgement v

1 Introduction 1

1.1 Background 1
1.2 Quantum Radar 3
1.3 Thesis overview 6

2 Quantum Theory 7

2.1 Introduction to quantum 7
2.2 Quantising the electromagnetic field 8
2.2.1 Classical electromagnetics 8
2.2.2 The harmonic oscillator 9
2.2.3 Quantised electromagnetics 10
2.2.4 Multimode light 11
2.3 Gaussian quantum states 12
2.3.1 Single-mode states 12
2.3.2 Two-mode states 14
2.4 Interacting with a noisy environment 16
2.4.1 Attenuation 16
2.4.2 Amplification 17

3 Metrology and Inference 19

3.1 Detection theory 19
3.1.1 Binary hypothesis testing 19
3.1.2 Likelihood ratio test 20
3.1.3 Quantum Illumination 21
3.1.4 QI with Asymmetric priors 23
3.2 Estimation theory 24
3.2.1 Quantum Fisher Information 25

4 Publications **27**
4.1 Paper I 27
4.2 Paper II 31
4.3 Paper III 33

5 Conclusion and Outlook **37**

A Appendix **41**
A.1 Computing Gaussian Quantum Fisher Information 41

Bibliography **48**

Paper I A comparison between quantum and classical noise radar sources **49**

Paper II Quantum Radar - What is it good for? **57**

Paper III Gaussian quantum estimation of the loss parameter in a thermal environment **65**

1

Introduction

I know the kings of England,
and I quote the fights historical;
From Marathon to Waterloo,
in order categorical;

Major-General Stanley in the opera
The Pirates of Penzance
by W.S. Gilbert and A. Sullivan

1.1 Background

The concept of actively using electromagnetic waves as a tool for surveying one's surroundings was demonstrated already in 1904 by Christian Hülsmeyer, when he used his invention of the *Telemobiloskop* to detect passing ships on the river Rhine [1, 2]. Famously, Hülsmeyer failed to interest the Navy in this invention, as they did not see an immediate use case, and the ideas of lay dormant for a few decades. It was during the 1930s and the lead-up to the second world war that radar systems found widespread use. This time, rapid development was motivated by the need to detect incoming aeroplanes at long ranges to increase the time available to react. Since those early days, radars have come a long way, with applications not only across many military disciplines, but also in civil sectors, such as air traffic surveillance, ship navigation and weather measurement. In fact, large parts of the electromagnetic spectrum have been realised for sensors, such as lasers, X-rays, infrared, not to understate the use of visual light that our eyes naturally use to survey our own surroundings.

A radar operates by transmitting electromagnectic waves into the environment and 'listening' for echoes generated by the reflection off of objects. Its operation is described directly in the name, as RADAR is an acronym for RAdio Detection and Ranging, referring to the use of radio waves to detect, and estimate properties of, objects, or *targets*. Although many systems today use the higher frequency microwaves in favour of radio waves, the term MIDAR, for MIcrowave Detection and Ranging, would be more fitting, but we describe also these systems as radars. To perform well and be able to detect targets at long distances, the radar must transmit a large amount of energy, because the fraction of energy reflected off of targets that is received back at the radar scales very unfavourably with the distance. Small targets would be covered by noise without sufficiently strong probing signals. A lot of signal processing techniques go into determining whether a received signal consists of only noise, or additionally a reflected copy of the transmitted signal, that is, a problem best approached with the statistical theory of *detection*.

At the same time as Hülsmeyer performed his prototype radar experiment, the first steps were taken in developing what would become known as modern physics, where quantum mechanics plays an important part. Understanding that the electromagnetic field, as described by Maxwell [3], needs to consist of individual quanta, was one of those insights. Today, we say that the quantized electromagnetic field consists of photons.

As time progressed, theories were developed to understand not only how quantum systems behave, but also their metrological properties [4]. Here, we refer to a system's ability to be used as a measurement probe in a sensor. This can be understood as follows. An experimentalist prepares a known probe and allows it to interact with an unknown system, and by measuring the outcome of the interaction, the experimentalist learns something about the unknown system. Fundamentally, these types of experiments are prone to some amount of error, not only due to calibration errors and measurement noise, but even in the ideal case, due to the uncertainties mandated by quantum mechanics. In many real-life applications, noise and other errors overwhelm the quantum mechanical uncertainties, but for specialized setups, proper understanding of these phenomena is of central importance if a naïve application of purely classical physics would lead to incorrect predictions. However, with careful analysis, adherence to quantum mechanics and a well-tuned experimental setup one may tweak the conditions to do better than any purely classical probe. These concepts may be collectively referred to as quantum enhanced sensing. Technical protocols enabled by quantum enhanced sensing have been developed, *e.g.*, to enhance the precision in detection of gravitational waves in the next generation of LIGO [5, 6]. Systems achieving this enhanced precision are said to beat the "standard quantum limit" (SQL) and exhibit quantum *advantage* over classical probes [7].

For the modern practical radar applications of today, a classical (as in non-quantum) description of electromagnetics is usually sufficient to understand the underlying physics, because the relevant energies vastly overwhelm the scale of individual photons. However, inspired by the potential benefits in harnessing the underlying quantum phenomena, there have been research efforts applied towards developing quantum radars. The recurring topic of this thesis and the appended papers is the study of when and how the unique properties of quantum mechanics can provide some benefit to radar-like scenarios and operation. In particular, the setting studied is one where a probe state is transmitted into a noisy environment to learn something from what comes back.

1.2 Quantum Radar

To say anything about quantum radar we need to acknowledge that there is no widely accepted meaning as what it should entail, whether it refers to an abstract theoretical protocol or a physical device, and the term can refer to different things depending on the context [8–10]. Going by the patented device described in Ref. [11], it can mean a radar system that uses "*a signal including a plurality of entangled particles*" for the purpose of resolving targets better than a classical system, by circumventing the Rayleigh diffraction limit. Another patented device, described in Ref. [12], uses a pair of entangled signals to realise a quantum advantage over a classical benchmark with the protocol of Quantum Illumination (QI). These patents indicate an interest not only from researchers, but also from the defence industry in these topics, and some of the patent authors were involved in a DARPA project on quantum sensors [13]. While that application was focused on LADAR[1], the underlying theory of quantum electromagnetics is the same, regardless of the frequency range. In the DARPA report, three types of quantum sensor are defined: Type-1, using non-classical probes that are not entangled to anything, Type-2, using classical probes, but a non-classical receiver, and Type-3, using probes that are entangled with the receiver.

The aforementioned QI protocol was named so in Ref. [14], where, building on the work of Sacchi [15, 16], Lloyd presented a method where an entangled signal-idler pair could significantly outperform single-photon signals serving as a benchmark, when the task is to discriminate whether a weakly reflecting target is present in a noisy background. This means QI is a Type-3 protocol, as defined in Ref. [13]. The signal-to-noise ratio (SNR) advantage over a single-photon probe i of Lloyd's protocol is exponential in the amount of entanglement. Extensions of the analysis to multi-photon signals showed that the performance of Lloyd's QI could be matched and even overtaken by a weak coherent state probe [17] . However, further development of the theory of target detection for Gaussian states by Tan *et al.* in Ref. [18] showed that, when comparing to the classical reference states, the possible entanglement advantage achieved in the effective SNR is not exponential, but a factor of 4, commonly referred to as "the 6 dB advantage". Although this result appears to restrict the situations where entangled signals are applicable compared to the earlier results of Lloyd, the QI protocol is particularly interesting from a purely theoretical point of view. This is because of the peculiar feature that QI uses an initially entangled pair of signals, but a quantum advantage is achieved over the classical benchmark even though the initial entanglement does not survive the probing process. It thus calls into question what role entanglement

[1] LADAR: LAser Detection and Ranging

has as a metrological resource. We will return to the QI protocol in Chapter 3, where it is described in more technical detail and the nature of the quantum advantage is discussed. For now, we continue with an informal overview presenting some of the related literature on QI and its interpretation as a quantum radar. It is important to note that although QI performs the detection part of radar operation, it actually requires prior knowledge of the transmit-to-receive path length to achieve any advantage. That is, the protocol does not measure time-of-flight, and is thus not able to perform detections at an unknown distance, omitting the Ranging part of radar. Nevertheless, the QI protocol has been understood as a type of quantum radar [8]. There are other protocols claiming to be quantum radars, where estimation of time-of-flight is incorporated [19].

A metrological protocol such as QI describes not only the probe state and measurement scenario, but also the receiver setup that measures the optimal observable. For the QI protocol, receiver structures based on Optical Parametric Amplification (OPA) and Phase-Conjugation (PC), respectively, were described by Guha and Erkmen [20] which lead to the patent of Ref. [12]. These receivers are *sub*-optimal in the sense that they can realise a factor of 2 advantage in the effective SNR over a coherent state probe, but not the full possible advantage. A theoretical receiver structure realising the full advantage has been suggested, based on iteration of sum-frequency generation, as presented in Ref. [21], but experimental realisation of that concept is not yet possible.

A no-go result in the high-loss regime was shown by Nair, where no quantum advantage can be achieved over a coherent state if the discrimination is done against a vacuum background [22]. This is a regime well approximated by visual light at room temperature, exhibiting negligible ambient thermal noise. One consequence of this no-go result is that, for the quantum advantage to be realised, it requires the discrimination to be against a noisy background. At ambient room temperature conditions the visible light spectrum does not satisfy this requirement. This indicates that a natural application at visible light frequencies is illusive. However, one can imagine an adversarial scenario with a strong thermal light source blinding the receiver sensor, where the QI protocol could outperform a coherent state probe.

On the other hand, in the microwave regime (approximately 300 MHz to 30 GHz) noise is naturally present at room temperature, but the necessary technology, *e.g.*, number resolving photon detectors, is not developed as of yet. This conundrum was approached in Ref. [23], with the proposed solution of using an optomechanical interface to coherently convert photons between visual light frequencies and microwaves. The idea is to prepare the entangled signal-idler pair at optical wavelengths, downconvert the signal to microwaves and transmit it, with the receiver doing the same operations in reverse. This scheme allows for the generation and detection of entangled photons to be done at optical frequencies, where the necessary technology is available, while the probing is done with microwaves, where the background is noisy.

Around this point in time, it became popular among media, primarily those covering defence development, to write about quantum radar applications and realisations, see, *e.g.*, Refs. [24, 25]. These reports, targeting a non-expert audience, tended towards creative interpretations of the quantum properties, such as the role of quantum entanglement, and overstated the maturity of the technology. For example, the dubious statement that quantum radar could beat stealth optimised aircraft was picked up as a revolutionary new technological achievement [24]. Nevertheless, reports like these increased awareness of the ideas and likely influenced decisions leading to further research funding.

On the academic side, there have been several publications claiming experimental demonstration of the QI protocol, *e.g.*, Ref. [26]. These results have been challenged as to whether they fully realised the QI protocol [27] on the grounds that coincidence-counting setups do not fully exploit the initial entanglement, and the ideal measurement is difficult to realise. In 2015, the QI protocol was demonstrated with a sub-optimal OPA receiver [28]. More recently, another experimental demonstration was performed with optics and coincidence counting by England *et al.* [29], where a jamming laser was used to artificially add background photons to the detector, albeit not a thermal background. Similarly, Blakely *et al.* [30] presented results of performing a similar QI-like task for LIDAR[2] applications.

A variation on the QI protocol was put forward in Refs. [31, 32] with experimental results in the microwave regime with free-space propagation, showing how entangled signals could outperform correlated thermal noise signals, at the same probe energies. These results garnered some attention because the experiments showed a quantum advantage with a simple heterodyne detection scheme and the demonstrated protocols were described as a type of quantum *noise* radar. While the initial pre-print of Ref. [33], published as `arXiv:1908.03058` in 2019, presented similar results at that point in time, the final published version clarifies that ideal photon number detection is required to realise the advantage. The pre-print result was also reported as a quantum radar [34]. Criticism as to the correctness of these results in the microwave regime as implementations of QI were raised by Shapiro in Ref. [27], where one of the main arguments is that the correlated thermal noise used as a classical reference system is not optimal and that, with minor modifications, the classical reference system would perform equivalently to the quantum enhanced system, and that measuring the signal and idler separately should destroy the QI advantage. Recently, a microwave experiment was reported, where also the joint measurement could be realised and a quantum advantage claimed [35]. Recently, alternative receiver structures have also been developed, utilising a transformation from signal-idler correlations to idler displacement [36, 37], which may be easier to implement as a sequential protocol [38].

[2]LIDAR: LIght Detection And Ranging

There are protocols other than QI that seek to exploit quantum properties in radar-like tasks [39], such as increasing measurement accuracies of distance with pulse compression [40] and velocity with Doppler shift [41], in addition to extensions to the target model, such as a target cloaking by phase-shifting the illuminating radiation [42] or when the target signal fluctuates over the observation interval [43]. There have also been some investigations into QI with three-mode entangled Gaussian states [44].

Within this thesis, we understand the term quantum radar as any device that uses features unique to quantum mechanics to gain an advantage over a classical or semi-classical counterpart, when transmitting the same total energy. However, the QI protocol and associated theory serves as the primary incarnation of quantum radar. The classical radars used as benchmarks are not to be confused with conventional radar systems, but rather as abstract devices that achieve the limit of what is possible with a non-quantum device. The prospects of real-life application of these quantum radars tend to lean towards close-range probing, such as a non-invasive scanning of sensitive samples, rather than competing with conventional radars that can find targets at ranges of up to hundreds of kilometres.

1.3 Thesis overview

The rest of the thesis is organized as follows. Chapter 2 presents a brief introduction to the essentials of quantum mechanics, and then moves on to describe the quantisation of the electromagnetic field, where Bosonic creation and annihilation operators are introduced. A particular set of relevant quantum states, referred to as ‘Gaussian’ are then presented, with focus on the single- and two-mode states that have been studied extensively for quantum radar. Then, a description of the dynamics of these states is summarized for the case where the interaction takes place with thermal systems. After this, Chapter 3 describes the setting of metrology and the task of *inference* and the methods one can apply to systematically learn something from statistical outcomes. Chapters 2 and 3 collectively present the theory toolbox that is central to the appended papers. For this text, the theory is kept at a somewhat simplified and informal description to efficiently convey the main ideas, rather than all the details. Conversely, the appended publications, and especially the third paper, follow a higher level of mathematical rigour. Chapter 4 quickly summarizes the main results and motivation of the appended papers. Two of the papers address questions about the use of correlated thermal noise as a classical reference, the applicability of QI for conventional radar operation and technological possibilities of QI. The third paper shifts focus to the task of estimation rather than discrimination, within a scenario that is similar to that of QI. Finally, an Outlook is presented in Chapter 5.

2

Quantum Theory

I'm very well acquainted, too,
with matters mathematical;
I understand equations,
both the simple and quadratical;

Major-General Stanley in the opera
The Pirates of Penzance
by W.S. Gilbert and A. Sullivan

2.1 Introduction to quantum

Simply described, a radar operates by transmitting electromagnetic waves, and finds objects in the environment by picking up reflected waves. To understand how this can be described in a setting where quantum effects are relevant, we thus need to describe the electromagnetic field in a manner that is compatible with quantum mechanics. This field of quantum electromagnetics is well established since many decades, and the overview presented here can be skipped by the reader familiar with the topic.

Before we go into detail on how the electromagnetic field is quantised and how we can study photons in radar-like scenarios, we need to set some ground rules by introducing the agents and the playing field of quantum mechanics. Shortly put, quantum mechanics is the framework that governs physical dynamics at small scales, such as for atoms and molecules. In quantum mechanics, the quantities are described mathematically in terms of states and operators that evolve under a dynamical relation – the Schrödinger equation. Our focus will mainly be on *mixed* states, described by the density operator ρ, which describe statistical ensembles. All the dynamics of a quantum mechanical system is described by the time evolution of the density operator.

An important axiom of quantum mechanics tells us how to get classical statistics out of the density operator. Without going into details, a 'measurement' that gives rise to an observation ω is described by the operator[1] Π_ω. A classical probability distribution is recovered from a quantum state as $p(\omega) = \mathrm{tr}\,\hat{\Pi}_\omega \rho$, known as the Born rule. The set of all measurements must resolve the identity, $\sum_\omega \hat{\Pi}_\omega = \hat{\mathbb{I}}$, which is simply a statement of conservation of probability. Importantly, one can imagine the task of an optimised experimental setup, where the measurement procedure is constructed to minimise the variance of the result. We return to this concept in the next chapter.

2.2 Quantising the electromagnetic field

Now, we sketch in an informal manner how electromagnetics can be made compatible with quantum mechanics as it is treated in quantum optics. This follows closely how the material is presented in textbooks, *e.g.*, Refs. [45, 46]. For a more rigorous derivation, see, *e.g.*, Ref. [47]. Throughout this thesis, we use natural units such as the reduced Planck constant ($\hbar = 1$) and the speed of light ($c = 1$), unless stated otherwise. In short, our goal is to promote the electric field $\mathbf{E}$ to a quantum mechanical operator $\hat{E}$, and to understand some of the implications.

2.2.1 Classical electromagnetics

We start by recalling Maxwell's equation in terms of the scalar potential ϕ and the vector potential $\mathbf{A}$ such that the free-space electric field is determined by $\mathbf{E} = -\nabla\phi - \partial_t \mathbf{A}$ and the magnetic field is determined by $\mathbf{B} = \nabla \times \mathbf{A}$. Then, the Maxwell equations for the potentials are

$$\nabla^2 \phi + \nabla \cdot \partial_t \mathbf{A} = -\boldsymbol{\sigma}, \tag{2.1}$$

$$\nabla(\nabla \cdot \mathbf{A}) - \nabla^2 \mathbf{A} + \partial_t \nabla\phi + \partial_t^2 \mathbf{A} = \mathbf{J}, \tag{2.2}$$

where $\boldsymbol{\sigma}$ and $\mathbf{J}$ are the charge and current density, respectively. The non-relativistic quantisation is more easily approached in the Coulomb gauge, with $\nabla \cdot \mathbf{A} = 0$, which simplifies the equations. Finally, by separating the current density into transverse and longitudinal components, $\mathbf{J} = \mathbf{J}_\mathrm{T} + \mathbf{J}_\mathrm{L}$, with $\nabla \cdot \mathbf{J}_\mathrm{T} = 0$ and $\nabla \times \mathbf{J}_\mathrm{L} = 0$, we get, in this gauge, that

$$\nabla^2 \phi = -\boldsymbol{\sigma}, \tag{2.3}$$

$$\partial_t \nabla \phi = \mathbf{J}_\mathrm{L}, \tag{2.4}$$

$$-\nabla^2 \mathbf{A} + \partial_t^2 \mathbf{A} = \mathbf{J}_\mathrm{T}. \tag{2.5}$$

Thus, we have a separation where electrostatics are determined by $\boldsymbol{\sigma}$ and $\mathbf{J}_\mathrm{L}$ through the scalar potential, while the electromagnetic waves are given by $\mathbf{J}_\mathrm{T}$ through the vector potential.

Now, we continue with the transverse Eq. (2.5) alone, and consider the free field where $\mathbf{J}_\mathrm{T} = 0$. This results in the wave equation for $\mathbf{A}$, as $-\nabla^2 \mathbf{A} + \partial_t^2 \mathbf{A} =$

[1] Most generally, a positive operator-valued measure.

0, which we subject to periodic boundary conditions of a 'big box' with side length L. Now, expand the vector potential at position $\mathbf{R}$ and time t in modes of wavevectors $\mathbf{k}$ and polarization $\boldsymbol{\pi} = \pm 1$ such that $\mathbf{A}(\mathbf{R}, t) = \sum_{\mathbf{k},\boldsymbol{\pi}} \vec{e}_{\mathbf{k}\boldsymbol{\pi}} \mathbf{A}_{\mathbf{k}\boldsymbol{\pi}}(\mathbf{R}, t)$, where $\mathbf{A}_{\mathbf{k}\boldsymbol{\pi}}(\mathbf{R}, t) = \mathbf{a}_{\mathbf{k}\boldsymbol{\pi}}(t)\mathrm{e}^{\mathrm{i}\mathbf{k}\cdot\mathbf{R}} + \mathbf{a}^*_{\mathbf{k}\boldsymbol{\pi}}(t)\mathrm{e}^{-\mathrm{i}\mathbf{k}\cdot\mathbf{R}}$ and where $\vec{e}_{\mathbf{k}\boldsymbol{\pi}}$ are the basis vectors. The boundary conditions require that $\mathbf{k} = \frac{2\pi}{L}(n_x, n_y, n_z)^\top$, with $n_x, n_y, n_z \in \mathbb{Z}$. This results in the harmonic oscillator equation

$$\partial_t^2 \mathbf{a}_{\mathbf{k}\boldsymbol{\pi}}(t) + \omega_k^2 \mathbf{a}_{\mathbf{k}\boldsymbol{\pi}}(t) = 0, \tag{2.6}$$

with frequency $\omega_k = |\mathbf{k}|$, for each field amplitude. The quantised frequencies are strictly a consequence of the periodic boundary conditions and are purely classical. The central step of quantising the field is to impose the quantum harmonic oscillator to Eq. (2.6) and to promote the mode fields to operators. Whenever possible, we drop the mode subscript $\mathbf{k}\boldsymbol{\pi}$ from now on, since the later analysis in the appended papers is not concerned with the exact nature of the modes.

2.2.2 The harmonic oscillator

The harmonic oscillator is the linear theory of oscillation. As a quick orientation, we quickly look at the classical harmonic oscillator. Assume a particle with mass m is affected by forces linear in generalized displacement q with some spring constant κ. The Hamiltonian of this classical harmonic oscillator is

$$H = \frac{p^2}{2m} + \frac{\kappa q^2}{2}, \tag{2.7}$$

where the canonical conjugate momentum is $p = m\dot{q}$. Applying the Hamilton equations of motion [48], $\dot{q} = \partial_p H$ and $\dot{p} = -\partial_q H$ gives the equation of motion as $\ddot{q} + \omega^2 q = 0$, where $\omega^2 = {}^{\kappa}/_{m}$. The general solution for q is

$$q(t) = c_- \mathrm{e}^{-\mathrm{i}\omega t} + c_+ \mathrm{e}^{\mathrm{i}\omega t}, \tag{2.8}$$

where the constants $c_+, c_- \in \mathbb{C}$ are determined by initial conditions. This solution describes harmonic periodic motion with the radial frequency ω.

The *quantum* harmonic oscillator can be introduced with the Hamiltonian operator

$$\hat{H} = \frac{1}{2}\left(\hat{q}^2 + \hat{p}^2\right), \tag{2.9}$$

where $\hat{q}$ and $\hat{p}$ are now Hermitian quantum operators in suitable units. Promoted to operators, the position and momentum satisfy the commutation relation $[\hat{q}, \hat{p}] = \hat{\mathbb{I}}\mathrm{i}$. The non-commuting nature of these conjugate operators implies that the respective variances jointly satisfy the Heisenberg uncertainty relation

$$(\Delta q)^2 (\Delta p)^2 \geq \frac{1}{4}. \tag{2.10}$$

The quantum harmonic oscillator algebra is given with the Bosonic annihilation and creation operators $\hat{a}$ and $\hat{a}^\dagger$, satisfying the commutation relation $[\hat{a}, \hat{a}^\dagger] = \hat{\mathbb{I}}$.

The quantum harmonic oscillator is naturally represented in a Fock space with state vectors $|n\rangle$, where the index $n = 0, 1, 2, \ldots$ labels the occupation number. The operators $\hat{a}$ and $\hat{a}^\dagger$ are also referred to as ladder operators, for their action on the Fock state $|n\rangle$, as $\hat{a}\,|n\rangle = \sqrt{n}\,|n-1\rangle$ and $\hat{a}^\dagger\,|n\rangle = \sqrt{n+1}\,|n+1\rangle$, 'stepping' up and down between states with different occupation numbers. This also invites the use of the number operator $\hat{N} = \hat{a}^\dagger\hat{a}$, for which $|n\rangle$ is an eigenstate: $\hat{N}\,|n\rangle = n\,|n\rangle$. The ladder operators are related to the position and momentum operators of the oscillator by the relations

$$\hat{q} = \frac{1}{\sqrt{2}}\left[\hat{a}^\dagger + \hat{a}\right], \tag{2.11}$$

$$\hat{p} = \frac{\mathrm{i}}{\sqrt{2}}\left[\hat{a}^\dagger - \hat{a}\right], \tag{2.12}$$

Rewriting the Hamiltonian operator of Eq. (2.9) in terms of the ladder operators and simplifying yields

$$\hat{H} = \hat{N} + \frac{1}{2}. \tag{2.13}$$

That is, for the Fock state $|n\rangle$, the expectation value of the Hamiltonian reads $\langle\hat{H}\rangle = n + \frac{1}{2}$. This additional term of $\frac{1}{2}$ tells us that even the state with occupation number zero has finite energy. This special minimum energy state, $|0\rangle$, exhibits vacuum fluctuations.

2.2.3 Quantised electromagnetics

Now that we are familiar with the harmonic oscillator, we can go back to Eq. (2.6) and take the solution $\mathbf{a}_{\mathbf{k}\boldsymbol{\pi}}(t) = \mathbf{a}_{\mathbf{k}\boldsymbol{\pi}}\mathrm{e}^{-\mathrm{i}\omega_k t}$. The field coefficient is now promoted to a quantum operator, as $\mathbf{a}_{\mathbf{k}\boldsymbol{\pi}} \to \hat{a}_{\mathbf{k}\boldsymbol{\pi}}$, where $\hat{a}_{\mathbf{k}\boldsymbol{\pi}}$ takes the role of a Bosonic annihilation operator and the occupation number n of the Fock state $|n\rangle$ refers to the number of photons that are contained in the mode. Now, we introduce a new phase $\gamma = \omega t + \mathbf{k}\cdot\mathbf{R}$ and again drop the subscript $\mathbf{k}\boldsymbol{\pi}$. Then, as an operator, the electric field is

$$\hat{E}(\gamma) = \frac{E_\omega}{\sqrt{2}}\left(\hat{a}\mathrm{e}^{-\mathrm{i}\gamma} + \hat{a}^\dagger\mathrm{e}^{\mathrm{i}\gamma}\right) \tag{2.14}$$

where E_ω is the electric field amplitude of one photon with frequency ω. If the field is measured in units of $E_\omega = 1$, all relations are simplified. Rewriting the electric field operator in terms of the generalized position and momentum with the relations of Eq. (2.11) and Eq. (2.12) yields

$$\hat{E}(\gamma) = \hat{q}\cos\gamma + \hat{p}\sin\gamma. \tag{2.15}$$

That is, the operators $\hat{q}$ and $\hat{q}$ take the role of *quadratures*. For the purposes of this thesis, we take $\hat{q}$ to be the in-phase component and $\hat{p}$ to be the orthogonal component, and refer them jointly as quadratures.

2.2.4 Multimode light

Even though we omit the explicit operator subscript that labels the wavenumber and polarization, it is nevertheless important to introduce a joint notation for states that consists of several modes, *e.g.*, $|n_1\rangle \otimes |n_2\rangle \otimes \ldots \otimes |n_N\rangle$. If such multimode-states are considered, we collect the quadratures in the vector[2] $\hat{r} = (\hat{q}_1, \hat{p}_1, \hat{q}_2, \hat{p}_2, \ldots, \hat{q}_N, \hat{p}_N)^\top$, such that the commutation reads $[\hat{r}_i, \hat{r}_j] = \mathrm{i}\boldsymbol{\Omega}_{i,j}$, for $\boldsymbol{\Omega} = \bigoplus_{j=1}^{N} \left(\begin{smallmatrix} 0 & 1 \\ -1 & 0 \end{smallmatrix}\right) = \mathbb{I}_N \otimes \left(\begin{smallmatrix} 0 & 1 \\ -1 & 0 \end{smallmatrix}\right)$. The matrix $\boldsymbol{\Omega}$ is the *symplectic form* and will appear again later in this chapter.

By expanding the quantisation to the continuum by taking the limit of $L \to \infty$, we can label the operators by the continuous frequency ω, as $\hat{a}_k \to \hat{a}(\omega)$. Then it makes sense to introduce time domain operators as Fourier transforms of frequency space operators

$$\hat{a}(t) = \frac{1}{\sqrt{2\pi}} \int_{-\infty}^{\infty} \mathrm{d}\omega\, \mathrm{e}^{\mathrm{i}\omega t} \hat{a}(\omega). \tag{2.16}$$

For some applications, such as light pulses, it is useful to use the formalism with photon-wavepacket operators

$$\hat{a}_\xi = \int_{-\infty}^{\infty} \mathrm{d}t\, \xi(t) \hat{a}(t) \tag{2.17}$$

for a pulse shape ξ. If we consider an orthonormal set of pulses[3] $\{\xi_i(t)\}_{i=1,2,\ldots}$, we retain a commutation relation as $\left[\hat{a}_{\xi_i}, \hat{a}^\dagger_{\xi_j}\right] = \hat{\mathbb{I}}\delta_{i,j}$. The frequency space operators are similarly related by inserting the expression of Eq. (2.16) and exchanging the order of integration, we get

$$\begin{aligned} \hat{a}_\xi &= \frac{1}{\sqrt{2\pi}} \int_{-\infty}^{\infty} \mathrm{d}t\, \xi(t) \int_{-\infty}^{\infty} \mathrm{d}\omega\, \mathrm{e}^{\mathrm{i}\omega t} \hat{a}(\omega) \\ &= \frac{1}{\sqrt{2\pi}} \int_{-\infty}^{\infty} \mathrm{d}\omega\, \hat{a}(\omega) \int_{-\infty}^{\infty} \mathrm{d}t\, \mathrm{e}^{\mathrm{i}\omega t} \xi(t) \\ &= \int_{-\infty}^{\infty} \mathrm{d}\omega\, \hat{a}(\omega) \zeta(\omega), \end{aligned} \tag{2.18}$$

where

$$\zeta(\omega) = \frac{1}{\sqrt{2\pi}} \int_{-\infty}^{\infty} \mathrm{d}t\, \mathrm{e}^{\mathrm{i}\omega t} \xi(t). \tag{2.19}$$

That is, a mode defined for a timed pulse with shape $\xi(t)$ can be expressed with the spectrum $\zeta(\omega)$, which is the Fourier transform of the pulse. When discussing radar-like applications, these are the types of modes that are understood to be used, even though a simplified notation is maintained.

[2] Another common ordering is $\hat{s} = (\hat{q}_1, \hat{q}_2, \ldots, \hat{q}_N, \hat{p}_1, \ldots, \hat{p}_N)^\top$. For this convention the symplectic form is $\boldsymbol{\Omega} = \left(\begin{smallmatrix} 0 & 1 \\ -1 & 0 \end{smallmatrix}\right) \otimes \mathbb{I}_N$.

[3] A set of pulse shapes such that $\int_{-\infty}^{\infty} \mathrm{d}t\, \xi_i(t) \xi_j^*(t) = \delta_{i,j}$.

2.3 Gaussian quantum states

Gaussian states are a particular set quantum mechanical states that find large use in quantum optics, both because of the convenient structure that allows for analytical treatment, and also because they can be readily prepared in the laboratory. There are many areas of applications for Gaussian states, beyond the scope of this thesis, see, *e.g.*, Ref. [49]. The theory presented here is primarily based on the review of Ref. [50] and the book of Ref. [51].

Similarly to random variables distributed according to the multivariate normal distribution, the Gaussian states are completely characterized by first order moment (or mean, μ) and second order moment (or covariance matrix, $\mathbf{\Sigma}$). The mean vector has elements $\mu_i = \langle \hat{r}_i \rangle$ and the covariance matrix has elements

$$\mathbf{\Sigma}_{kl} = \frac{1}{2} \langle \hat{r}_k \hat{r}_l^\dagger + \hat{r}_l^\dagger \hat{r}_k \rangle - \langle \hat{r}_k \rangle \langle \hat{r}_l^\dagger \rangle . \tag{2.20}$$

In many places of the literature, *e.g.*, Ref. [51], one finds the rescaled covariance matrix $\sigma = 2\mathbf{\Sigma}$, which simplifies some expressions. In **Paper I**, we encounter a normalised version of the covariance matrix, denoted as the matrix *correlation* coefficients, which can be computed as

$$\mathbf{r} = [\mathrm{diag}(\mathbf{\Sigma})]^{-1/2}\, \mathbf{\Sigma}\, [\mathrm{diag}(\mathbf{\Sigma})]^{-1/2}. \tag{2.21}$$

While the correlation coefficients by themselves are insufficient to characterize the state, they appear as the relevant quantity in one of the discrimination tasks studied in **Paper I**.

For Gaussian states, the non-commuting property of conjugate quadratures gives rise to an uncertainty relation that can be cast as a criterion on the covariance matrix

$$\mathbf{\Sigma} + \mathrm{i}\mathbf{\Omega}/2 \succeq 0, \tag{2.22}$$

where $\mathbf{\Omega}$ is the symplectic form. This is known as the Robertson-Schrödinger uncertainty relation.

2.3.1 Single-mode states

The single-mode Gaussian states can be parametrized in terms of a 2×1 mean vector and a 2×2 covariance matrix. In this section, we present some particular states as well as the canonical generic Gaussian single-mode state. Here, without loss of any generality, we use a reference phase such that the covariance matrix is diagonal. A special state is the minimum energy *vacuum* state denoted by $|0\rangle$, with zero mean and covariance matrix $\mathrm{diag}\left(\frac{1}{2}, \frac{1}{2}\right)$. The vacuum contains zero photons on average, but non-zero variance, which can be understood in terms of quantumness as consequence of the uncertainty principle applied to the quadratures. That is, the state containing zero photons has a minimum variance of $\frac{1}{2}$ for both quadratures and this defines the standard quantum limit (SQL). If a state can achieve a measurement variance lower than $\frac{1}{2}$, it is said to 'beat' the SQL and that it exhibits some quantum advantage.

Coherent State

If we take the vacuum state and change the mean to be non-zero, we find the *coherent state*, which is the eigenstate of the annihilation operator. That is, for a coherent state $|\alpha\rangle$ labelled by the complex parameter $\alpha \in \mathbb{C}$, the state satisfies $\hat{a}\,|\alpha\rangle = \alpha\,|\alpha\rangle$. The average number of photons of the coherent state is $\langle \hat{N} \rangle = |\alpha|^2 = N_{\mathrm{coh}}$. This means that the coherent state can also parametrized with $\alpha = \sqrt{N_{\mathrm{coh}}}\mathrm{e}^{\mathrm{i}\phi}$, for a phase $\phi \in [0, 2\pi)$, as

$$\mu = \sqrt{2}\begin{pmatrix} \mathfrak{Re}\,(\alpha) \\ \mathfrak{Im}\,(\alpha) \end{pmatrix}, \tag{2.23}$$

$$\mathbf{\Sigma} = \frac{1}{2}\begin{pmatrix} 1 & 0 \\ 0 & 1 \end{pmatrix}. \tag{2.24}$$

In some sense, the coherent state behaves as a classical state, describing the state produced by a monochromatic laser. For this reason it often serves as the classical benchmark to beat in a quantum enhanced protocol.

Thermal state

The thermal state is a zero-mean state with covariance matrix

$$\Sigma = \begin{pmatrix} N_{\mathrm{th}} + \frac{1}{2} & 0 \\ 0 & N_{\mathrm{th}} + \frac{1}{2} \end{pmatrix}. \tag{2.25}$$

This state is understood as the thermal equilibrium state at temperature T, where the number of photons N_{th} is given by the Bose-Einstein distribution at zero chemical potential, or $N_{\mathrm{th}} = \left(\mathrm{e}^{hf/k_{\mathrm{B}}T} - 1\right)^{-1}$, where f is the frequency, h is the Planck constant and k_{B} the Boltzmann constant. As an example, for a system operating with microwave frequencies at room temperature the thermal background is strong, with $N_{\mathrm{th}} \simeq 1000$, while for visible light $N_{\mathrm{th}} \simeq 0$, explaining why our eyes are not blinded by the environment. To have negligible thermal background at microwave frequencies, the ambient temperature has to be reduced to a few milliKelvin, and this can be achieved with dilution refrigerators.

Single-mode squeezed vacuum

As we have noted, even the semi-classical coherent state exhibits the quantum feature of a finite variance. For the coherent state and the vacuum state, this variance is symmetrically shared between the two quadratures. However, states can be prepared where this uncertainty is asymmetrically distributed. This is most easily understood as a transformation of the vacuum state, where the variance in one quadrature is reduced, while the orthogonal quadrature sees an increase in variance. In the covariance matrix, this can be parametrised as

$$\Sigma = \frac{1}{2}\begin{pmatrix} s & 0 \\ 0 & s^{-1} \end{pmatrix}, \tag{2.26}$$

with the squeezing parameter $s \in (0, \infty)$. Squeezing is an active process, adding $N_{\text{sq}} = \frac{1}{4}\left(s + s^{-1}\right) - \frac{1}{2}$ average photons to the vacuum.

Displaced squeezed thermal state

Finally, the generic single-mode Gaussian state consists of first squeezing a thermal state, and then displacing the mean. Applying squeezing to a state with non-zero displacement results in a non-Gaussian state, which we do not consider here. That is, we can characterize the canonical Gaussian state with mean and covariance matrix as

$$\mu = \begin{pmatrix} \bar{q} \\ \bar{p} \end{pmatrix}, \tag{2.27}$$

$$\Sigma = \begin{pmatrix} \left(N_{\text{th}} + \frac{1}{2}\right) s & 0 \\ 0 & \left(N_{\text{th}} + \frac{1}{2}\right) s^{-1} \end{pmatrix}, \tag{2.28}$$

where $N_{\text{th}} \geq 0$ is the number of thermal photons, $s \in (0, \infty)$ is again the squeezing and $\bar{q}, \bar{p} \in \mathbb{R}$ are the displacements. The total number of photons in this generic state is $N = N_{\text{coh}} + N_{\text{sq.th}} + N_{\text{th}}\left(2N_{\text{sq.th}} + 1\right)$. As can be seen, increasing the mean adds 'coherent' photons linearly, while the squeezing or changing the temperature of the thermal state adds photons non-linearly, with $N_{\text{sq.th}} = \frac{2N_{\text{th}}+1}{4}\left(s + s^{-1}\right) - \frac{1}{2}$.

2.3.2 Two-mode states

By introducing a second mode to the Gaussian states, the mean vector is now of size 4×1 and the covariance matrix is of size 4×4. This means that a generic two-mode Gaussian system has 14 free parameters. The appended **Paper III** considers various symmetries and constraints to reduce the number of free parameters for a certain type of problem. Here, we neglect to state explicitly the fully generic two-mode state, and describe instead two special two-mode states in some detail.

Two-mode squeezed vacuum

An important non-classical feature that is introduced with two-mode states is that we can have *entanglement* between the modes. A state that exhibits entanglement is the two-mode squeezed vacuum state (TMSV). Actually, it is the *maximally* entangled two-mode state on a per-photon basis [49].

The TMSV state can be generated with parametric amplification of the vacuum, generating pairs of photons in two entangled modes denoted as *signal* and *idler*, respectively. If the two modes are separated, and the signal is used as probe in a metrological protocol, one can achieve entanglement-enhanced performance, which may surpass that of a purely classical probe on a per-photon basis. Because of the generation process of the TMSV state, the average number of photons in the signal and idler are equal, denoted N_S. Further, we can easily parametrise the TMSV state with zero mean and a covariance matrix

$$\mathbf{\Sigma}_{\text{TMSV}} = \begin{pmatrix} N_S + 1/2 & 0 & \sqrt{N_S(N_S+1)} & 0 \\ 0 & N_S + 1/2 & 0 & -\sqrt{N_S(N_S+1)} \\ \sqrt{N_S(N_S+1)} & 0 & N_S + 1/2 & 0 \\ 0 & -\sqrt{N_S(N_S+1)} & 0 & N_S + 1/2 \end{pmatrix}. \tag{2.29}$$

The statistics of each mode individually is indistinguishable from thermal noise, but the inter-mode covariance $\sqrt{N_S(N_S+1)}$ – being larger than the classical limit of N_S – reveals that the state exhibits non-classical correlations. These non-classical correlations are apparent in the regime with few photons per mode, $N_S \ll 1$, where $\sqrt{N_S(N_S+1)} \gg N_S$, while, in the strong signal regime, with $N_S \gg 1$, we have $\sqrt{N_S(N_S+1)} \simeq N_S$.

Correlated thermal noise

As a classical counterpart to the TMSV state, we can study the two-mode state consisting of correlated thermal modes, that we denote as classically correlated noise (CCN). This state has not been widely studied in literature, so we spend some time describing it. The CCN state is generated by mixing the noise from two independent thermal sources at temperatures T_H and T_C, described by the operators $\hat{a}_H$ and $\hat{a}_C$. Here, the subscripts H and C refer to 'hot' and 'cold', respectively, indicating that we take $T_H \geq T_C$. Each thermal source is in a state of single-mode thermal noise, with average number of thermal photons denoted by N_H and N_C, respectively.

The procedure of preparing the CCN state is illustrated in Fig. 2.1, where the two thermal sources are allowed to interact over a beamsplitter labelled by the variable reflection coefficient $\beta \in [0, 1]$. The output modes, also designated as signal and idler, are

$$\hat{a}_S^{\text{CCN}} = \sqrt{\beta}\hat{a}_H + \sqrt{1-\beta}\hat{a}_C, \tag{2.30}$$
$$\hat{a}_I^{\text{CCN}} = -\sqrt{1-\beta}\hat{a}_H + \sqrt{\beta}\hat{a}_C. \tag{2.31}$$

Being a Gaussian state, the CCN state is characterized by having a zero first order moment and the covariance matrix

$$\mathbf{\Sigma}_{\text{CCN}} = \begin{pmatrix} N_S + 1/2 & 0 & \gamma_{SI} & 0 \\ 0 & N_S + 1/2 & 0 & \gamma_{SI} \\ \gamma_{SI} & 0 & N_I + 1/2 & 0 \\ 0 & \gamma_{SI} & 0 & N_I + 1/2 \end{pmatrix}, \tag{2.32}$$

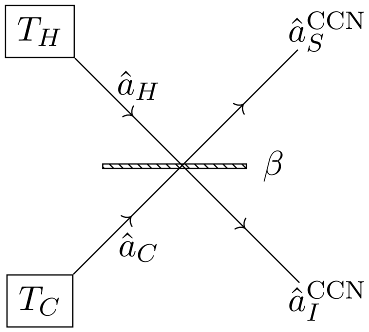

Figure 2.1: Overview of how two correlated thermal modes can be generated by mixing two independent thermal modes on a β-parametric beamsplitter. If the two thermal sources have different average number of photons $N_H \neq N_C$, the output modes will be correlated. [Reproduced from Fig. 1 of **Paper I**.]

where $N_S = \beta N_C + (1-\beta) N_H$, $N_I = (1-\beta) N_C + \beta N_H$, and $\gamma_{SI} = \sqrt{\beta(1-\beta)}(N_H - N_C)$. As long as the input modes have different number of photons on average, corresponding to different temperature, the output modes $\hat{a}_S^{\text{CCN}}$ and $\hat{a}_I^{\text{CCN}}$ are correlated.

2.4 Interacting with a noisy environment

Central to this thesis is the use of Gaussian states as signals to probe dynamical systems and learn something about their parameters. We restrict the dynamics to Gaussian-*preserving* interactions, where Gaussian states are mapped to Gaussian states.

2.4.1 Attenuation

While the discussion is quite general, we are particularly interested in radar-like scenarios, where the signal is transmitted into a noisy environment with N_B number of photons per mode, and there may be a small part of the signal coming back to the receiver.

For Gaussian states, these dynamics can be cast as a beamsplitter mixing the signal mode $\hat{a}_S$ with an environmental thermal noise mode $\hat{a}_B$. Then, the return mode that arrives at the receiver is given by

$$\hat{a}_R = \eta \hat{a}_S + \sqrt{1-\eta^2}\, \hat{a}_B \tag{2.33}$$

for a transmission coefficient given by $\eta \in (0,1)$, while the complementary mode is lost to the environment. A derivation of how this model represents the transmit-to-receive dynamics is given in Ref. [52]. The introduction of a thermal mode $\hat{a}_B$ is unavoidable for any $\eta < 1$ since the transformation needs to be unitary. The central problem in all of the appended papers is that the attenuation is unknown and the signal mode is used to measure it. To specify the problem of interest, we take the unknown transmission coefficient η to be identical over many repeated copies of probe state.

For a two-mode state, partitioned into signal and idler, this channel can be cast as a map of the mean and covariance matrix as

$$\begin{pmatrix} \bar{q}_S \\ \bar{p}_S \\ \bar{q}_I \\ \bar{p}_I \end{pmatrix} \to \begin{pmatrix} \eta\bar{q}_S \\ \eta\bar{p}_S \\ \bar{q}_I \\ \bar{p}_I \end{pmatrix}, \tag{2.34}$$

$$\begin{pmatrix} \Sigma_S & \Sigma_{SI} \\ \Sigma_{SI}^\dagger & \Sigma_I \end{pmatrix} \to \begin{pmatrix} \eta^2\Sigma_S + (1-\eta^2)\left(N_B + \frac{1}{2}\right)\mathbb{I} & \eta\Sigma_{SI} \\ \eta\Sigma_{SI}^\dagger & \Sigma_I \end{pmatrix}. \tag{2.35}$$

It is common to introduce a normalisation of the background noise, as $N_B \to N_B/(1-\eta^2)$. The normalisation removes the effect where measuring a background gives information of η, regardless of the signal mode, referred to as the 'shadow effect' [53]. This is done *ad hoc* to eliminate any metrological power of the background and isolate the effect of the signal. Intuitively, the normalised channel models a scenario where the target, if present, emits an average number of thermal photons that equals that of the background environment were the target absent.

2.4.2 Amplification

As an alternative to attenuation, one can study amplification of a mode. In the simplest possible model [54], a phase-insensitive amplifier transformation of the signal $\hat{a}_S$ can be written

$$\hat{a}' = \sqrt{G}\hat{a}_S + \sqrt{G-1}\hat{a}_B^\dagger, \tag{2.36}$$

where the amplifier power gain is $G \geq 1$. Just as for the attenuator channel, there is always a thermal mode $\hat{a}_B$ involved, to ensure that the transformation is unitary. Note that amplification, being an active process introduces a conjugation of the thermal noise mode, as compared to the passive attenuator channel above.

3

Metrology and Inference

About binomial theorem
I'm teeming with a lot o' news;
With many cheerful facts
about the square of the hypotenuse;

Major-General Stanley in the opera
The Pirates of Penzance
by W.S. Gilbert and A. Sullivan

3.1 Detection theory

As a subset of metrology, hypothesis testing forms the basis for most of quantitative science by systematically deciding which of a prescribed set of descriptions best fit observed data. Quantum mechanics sets the fundamental limits on how well any such method can be implemented for physical systems. While many quantitative fields can perform these inferences perfectly well without an in-depth understanding of quantum mechanics, there are fields where quantum features become relevant, see, *e.g.*, the relatively recent reviews of Refs. [7, 55] on quantum metrology.

3.1.1 Binary hypothesis testing

Assume that a measurement is made to register the signal level x, *e.g.*, a voltage. The question is whether x originates from ambient noise, or from a known signal plus the ambient noise. That is, we can state the problem as a binary decision where the two hypotheses are

$$\begin{aligned} \mathcal{H}_0 : &\quad x = \text{noise}, \\ \mathcal{H}_1 : &\quad x = \eta \cdot \text{signal} + \text{noise}. \end{aligned}$$

Here, η takes the role of a transmission coefficient, and $\eta = 0$ implies the null hypothesis $\mathcal{H}_0$. A detector can be defined as an abstract function that takes as input a set of observations and outputs a declaration as to which hypothesis best corresponds to the observed data. In the binary case, this can be understood as a threshold, where weak observations are declared for the null hypothesis and strong signals are declared for the alternate hypothesis. Regardless of what the threshold is tuned to, the detector will unavoidably be subject to statistical error. For any given problem, the detector can be characterized in terms of the conditional probabilities that it declares the correct (or false) result. In the context of radar, it is conventional to use the events of *True Positive* and *False Positive* outcomes, quantified as the probability of detection P_{D} and false alarm P_{FA}, respectively. Here, both detection and false alarm refers to the event of the detector declaring in favour of target presence, conditioned on whether the target is actually present or not. Equivalently, one can also study the complementary quantities of *False negative* and *True negative.* In the terminology of decision making, the false alarm is a Type-I error and the false negative is a Type-II error. A quantity familiar to any radar engineer is the relation between probability of detection and probability of false alarm, given a certain signal-to-noise ratio. This relation is known as a *Receiver Operating Characteristic* and captures how enforcing a low probability of false alarms by raising the threshold necessarily lowers the probability of detection.

As an alternative to studying the trade-off between the Type-I and Type-II errors, one can can minimise the related quantity of the total error probability, defined as

$$P_{\mathrm{E}} = \pi_0 P_{\mathrm{FA}} + \pi_1 \left(1 - P_{\mathrm{D}}\right), \tag{3.1}$$

where π_0 and π_1 are the *a priori* probabilities of the events associated with $\mathcal{H}_0$ and $\mathcal{H}_1$, respectively. The total error is commonly used in the communication scenario, where the priors are known and usually symmetric ($\pi_0 = \frac{1}{2} = \pi_1$). In radar, on the other hand, the prior probabilities are unknown and the total error probability is undefined.

3.1.2 Likelihood ratio test

One common and useful way to define a binary detector function when the priors are unknown is as a likelihood ratio test [56] (LRT). The LRT takes as input a set of observations $\mathbf{X} = \{x_1, x_2, \ldots, x_M\}$ and computes the test statistic L_G as the likelihood ratio and compares its value to a threshold. As a relation, this can be understood as

$$L_G = \frac{p_1(\mathbf{X} \,|\, \mathcal{H}_1)}{p_0(\mathbf{X} \,|\, \mathcal{H}_0)} > \tau, \tag{3.2}$$

where τ is the threshold. Here, p_i denotes the probability density function of $\mathbf{X}$ under hypothesis $\mathcal{H}_i$. For practical purposes, the log-likelihood test statistic, $\Lambda_G = 2 \log L_G$, is often more useful than the direct ratio. For example, it is known that, for many repeated independent and identically distributed measurements, such that the central limit theorem applies, any log-likelihood test is asymptotically

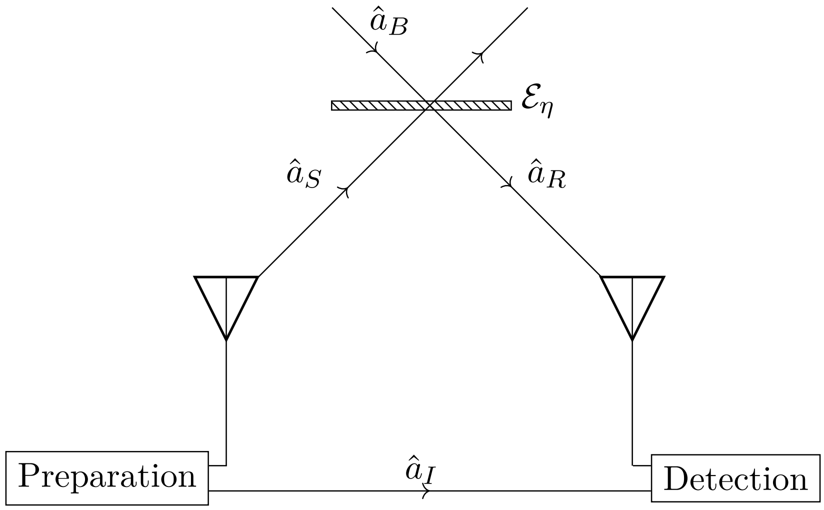

Figure 3.1: Schematic overview of the QI protocol. An entangled signal-idler pair is prepared. The signal mode $\hat{a}_S$ is sent to interact with an unknown channel $\mathcal{E}_\eta$, modelled as a lossy Bosonic channel. From the channel the return mode $\hat{a}_R$ is jointly measured with the retained idler $\hat{a}_I$, and a detection is declared if the detector finds sufficient statistical evidence that $\eta > 0$. Otherwise the detector stays silent. [Reproduced from Fig. 2 of **Paper I**.]

distributed as a chi-squared random variable. This result is known as Wilks's theorem [57].

For a *simple* binary hypothesis test, for example $\eta = \eta_0$ vs $\eta = \eta_1$, the likelihood ratio test is optimal by the Neyman-Pearson Lemma [56]. In a radar scenario, the simple hypothesis is usually not encountered, because the value of η is not known, and the discrimination is between hypotheses $\eta = 0$ and $\eta > 0$. In this case optimality of the likelihood ratio test is not guaranteed since $\eta > 0$ is not a simple hypothesis, but a *composite* hypothesis consisting in a continuous family of hypotheses. In the general case, is it impossible to find a globally optimal detector function for these problems, and one might have to resort to a locally optimised test.

3.1.3 Quantum Illumination

We now move on to the world of quantum detection theory, with a focus on the QI protocol, since it serves as the recurring foundation of quantum radar. As outlined here and in the Introduction, quantum illumination fundamentally fails to perform some of the tasks of a conventional radar protocol. It can be argued that QI is at best radar-like. As a protocol, QI performs the task of discriminating between two possible states in the following way: A probe ρ_{Pr} consisting of an entangled signal-idler pair in a TMSV state is generated. The signal, consisting of N_S number of photons on average, is passed through one of two possible channels. The channels are Bosonic lossy thermal noise channels injecting N_B noise photons on average,

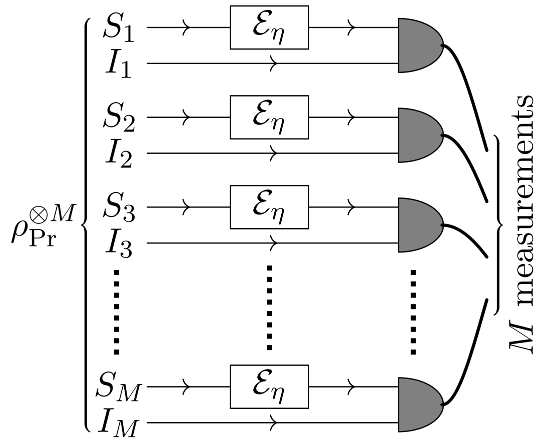

Figure 3.2: Illustration of M probes with respective entangled ancilla idlers are passed through the channel $\mathcal{E}_\eta$ and then measured separately. The most general protocol would jointly measure all $2M$ modes. [Reproduced from Fig. 1 of **Paper III**.]

see Section 2.4, with either no transmission $\eta = 0$ (the Null hypothesis, $\mathcal{H}_0$) or small, finite transmission $\eta = \eta_1$ with $0 < \eta_1 \ll 1$ (the Alternative Hypothesis, $\mathcal{H}_1$). Thus, both $\mathcal{H}_0$ and $\mathcal{H}_1$ are *simple* hypotheses. Back at the receiver we get either the state ρ_0 or the state ρ_1, corresponding to the respective hypotheses, see Figure 3.1. This test can be repeated independently for M modes, for example by frequency multiplexing, or by repetition over time. The final task is thus to discriminate between $\rho_0^{\otimes M}$ and $\rho_1^{\otimes M}$, and decide which channel was in effect during the measurement. This task is illustrated in Figure 3.2, for a receiver setup where each signal-idler pair is measured jointly, but the different pairs are measured separately. Since a sufficiently strong signal will outperform any weaker signal, a constraint imposed on the problem is that the average number of photons in the signal mode N_S is fixed.

As QI was developed for a symmetric binary hypothesis test, the priors are assumed equal and the protocol seeks to minimise the total error probability. The quantum Chernoff bound [58, 59] is the central result that enables this analysis. It says, informally, that, as the number of repeated trials M grows, the total error probability will asymptotically enter a regime where it is bounded from above by an exponentially decaying function, as $P_{\mathrm{E}} \leq \frac{1}{2}\mathrm{e}^{-M\xi_{\mathrm{C}}}$, where

$$\xi_{\mathrm{C}} = -\log\left(\min_{0\leq s\leq 1} \mathrm{tr}\left[\rho_0^s \rho_1^{1-s}\right]\right) \tag{3.3}$$

is the quantum Chernoff coefficient that determines the decay rate. It is in this situation that we can identify the Chernoff coefficient as the *error exponent*. Computation of ξ_{C} can be difficult and a more simpler approach is found by relaxing the inequality and computing instead the less tight Bhattacharrya bound with coefficient $\xi_{\mathrm{B}} \leq \xi_{\mathrm{C}}$. The Bhattacharrya coefficient[1] ξ_{B} is found from Eq. (3.3) by

[1]In the literature, one encounters the term of Bhattacharrya *distance* [60], favouring a geo-

neglecting the minimisation procedure and requiring instead $s = \frac{1}{2}$. It is in this context that Tan *et al.* [18] established that the Chernoff coefficient for a coherent state probe is $\xi_{\mathrm{C}}^{\mathrm{coh.}} = \frac{\eta_1 N_S}{4N_B}$ and the Bhattacharrya coefficient for a TMSV probe with an entangled idler is $\xi_{\mathrm{B}}^{\mathrm{TMSV}} = \frac{\eta_1 N_S}{N_B}$, *i.e.*, a factor of four advantage, or approximately 6 dB, in the regime where $N_S \ll 1$, $N_B \gg 1$ and $\eta_1 \ll 1$.

One might ask as to what extent the coherent state serves as a relevant classical benchmark. Maybe there are other classical states that perform better? The answer can be understood quite simply. Fundamentally, there are limits to how well the discrimination task can be performed for *any* probe state, see Ref. [61] which states that, for the noise-free regime, $N_B \simeq 0$, the coherent state saturates the fundamental limit. Conversely, for the noisy regime $N_B \gg 1$ the TMSV saturates the limit. This can further be understood as a no-go for any quantum advantage in the low-noise regime because no probe can do better than to match the coherent state performance.

The final aspect of any discrimination protocol is the description of a receiver structure that, ideally, realises the theoretical performance. That is, the measurement operator should be constructed. For example, the optimal strategy is not possible with local measurements [62] and a joint measurement strategy between the return mode and the idler is required. The OPA receiver with photon-counting and the PC receiver with balanced detection, both described in Ref. [20], realise only a sub-optimal factor of two in the error exponent. A receiver structure that *does* achieves the full factor of four advantage was described in Ref. [21], although building a device according to this scheme is technologically unfeasible. However, the existence of an optimal scheme, albeit as a theoretical concept, is still important for the understanding of the QI protocol. As a complement to working with asymptotic results and somewhat abstract tools, important work has also been done with the task of practical implementations and comparison with classical protocols, see Ref. [63].

An important feature of quantum illumination is that entangled state protocol presents a discrimination advantage over a non-entangled state, even though the entanglement itself does not survive through the channel. That is, the advantage should not be understood as a residual entanglement, but the interpretation is rather that the signal-idler correlations of the probe state are stronger than those of any possible separable state [18]. It has also been suggested that quantum discord is the relevant quantity underlying any advantage [64].

3.1.4 QI with Asymmetric priors

As noted earlier, in conventional radar it is customary to avoid introducing assumptions about any prior probabilities of the respective hypotheses. While the original development of the QI protocol was for symmetric priors, it has also been

metrical interpretation. Here, we use instead *coefficient* to keep the terminology consistent.

extended to the general case of unknown, possibly asymmetric priors, more in line with conventional radar operation [65, 66]. In this variation, the task is typically to maximise the probability of detection, while ensuring that the probability of false alarm is bounded by some prescribed rate ε, or finding the optimal probe state ρ^* such that

$$\rho^* = \underset{\substack{\rho \\ P_{\mathrm{FA}} \leq \varepsilon}}{\operatorname{argmax}} P_{\mathrm{D}}(\rho). \tag{3.4}$$

In this situation we can not rely on the Chernoff bound, but instead turn to the similar asymptotic result of Stein's Lemma [67, 68], which states that, for any ε, the probability of a missed detection is bounded as the number of repeated trials tends to infinity. Informally, we understand this mathematically as

$$1 - P_{\mathrm{D}} \leq \mathrm{e}^{-MD(\rho_1||\rho_0)}, \tag{3.5}$$

where $D(\rho_1||\rho_0) = \operatorname{tr} \rho_1 (\ln \rho_1 - \ln \rho_0)$ is the quantum relative entropy between the two possible output states. It has been shown that also in this scenario, the TMSV state is optimal [69], but the nature of the advantage is slightly more complicated than a single number, as it depends non-trivially on the scenario. In fact, as $N_S \to 0$, the advantage of a TMSV state probe over a coherent state grows without bound. While this would appear incredibly useful at first glance, due to the fact that the absolute discrimination strength goes to zero in the same limit, it is simply a result of the relative entropy tending to zero faster for the coherent state than for the TMSV state.

As Stein's Lemma is asymptotic, it does not depend on the choice of ε. Higher order asymptotic terms for the quantum Stein's Lemma have been developed by Li [70] and used to analyse the transition to asymptotic behaviour of QI in Ref. [65]. If we stick with the informal mathematical description, the semi-asymptotic Stein's Lemma takes the form

$$1 - P_{\mathrm{D}} \leq \mathrm{e}^{-MD(\rho_1||\rho_0) - \sqrt{MV(\rho_1||\rho_0)}\Phi^{-1}(\varepsilon)}, \tag{3.6}$$

where $V(\rho_1||\rho_0) = \operatorname{tr} \rho_1 [\ln \rho_1 - \ln \rho_0 - D(\rho_1||\rho_0)]^2$ is the relative entropy *variance*, and where Φ^{-1} is the inverse standard normal distribution. Note that $\Phi^{-1}(\varepsilon) < 0$ for $\varepsilon < \frac{1}{2}$, which means a smaller relative entropy variance is beneficial to the discrimination strength.

3.2 Estimation theory

As an alternative to the discrete decision problem, one can study the problem of estimation. Consider again the previous example of a voltage, where the task is now to estimate an unknown DC level subject to fluctuations from thermal noise. If the DC level is small with respect to the noise fluctuations, it is more difficult to determine its value with certainty.

For the case we have studied so far – a lossy Bosonic channel with an unknown transmission coefficient – this would correspond to the question "*What is the value of the unknown parameter* η?". Explicitly, we want to construct an *estimator*, *i.e.*, a function[2] $\tilde{\eta}$ that takes as input observations and outputs a numerical value that is the best guess of the true value of η. Since the estimator is a function of random data, it is itself a random variable. Therefore, it is important to characterize the statistics of the estimator in order to quantify its performance. A full characterization can be understood as all the statistical moments being known. However, for practical reasons it is often sufficient to determine only the first two moments, or, equivalently the average and variance. A particularly important example is when the estimation is done with a Gaussian noise background, where the first and second moments are sufficient to determine all the higher order moments. In our case of the thermal lossy Bosonic channel, the estimation is indeed done against Gaussian noise generated by a thermal state. We again imagine that the measurement of η can be performed for M independent trials, as indicated in Figure 3.2.

Central to the performance of any estimator is thus its variance, which should be minimal. However, one may inquire how small the variance could be for *any* estimator and define an a criterion of optimality if this minimum is saturated. The tool of this analysis is the Cramér-Rao lower bound (CRLB) [71] . For a classical estimation problem, CRLB is a result given in terms of a random variable X that is distributed according to the parametric probability density function $p_X(x;\eta)$. If we wish to estimate the value of η based on observations of X, the CRLB tells us that the minimum achievable variance of *any* (unbiased) estimator of η is given by

$$\operatorname{Var}\tilde{\eta} \geq (MI_\eta)^{-1}\,, \tag{3.7}$$

where

$$I_\eta = \mathbb{E}_X[(\partial_\eta \log p_X(x;\eta))^2] \tag{3.8}$$

is the Fisher information of η with respect to the random variable X. A large Fisher information indicates that the unknown parameter can be estimated with small variance.

3.2.1 Quantum Fisher Information

When moving from classical statistics to quantum mechanics, the task of estimation is further complicated by the introduction of different possible projective measurements, giving rise to different classical statistics.

The quantum Fisher information (QFI) [4] is defined, given the density operator ρ_η labelled by the continuous parameter η to be estimated, as the classical Fisher

[2] It is traditional notation to use hats $(\hat{\cdot})$ for estimators, but we refrain from it here to avoid confusion with quantum mechanical operators.

Information maximised over all possible measurements $\hat{\Pi}_\mu$, or

$$J(\rho_\eta) = \max_{\hat{\Pi}_\mu} I_\eta. \tag{3.9}$$

Thus, the QFI is manifestly the maximally achievable classical Fisher information, when the optimal measurement is implemented. Mathematically, the QFI can be computed as $J(\rho_\eta) = \mathrm{tr}\left[\rho_\eta \hat{\mathcal{L}}_\eta^2\right]$, where $\hat{\mathcal{L}}_\eta$ is the symmetric logarithmic derivative (SLD), implicitly defined by the condition $2\partial_\eta \rho_\eta = \{\hat{\mathcal{L}}_\eta, \rho_\eta\}$. An implementation of calculating the SLD of Gaussian states, suitable for use with computer algebra systems, is presented in Appendix A.

Given this definition of the QFI, the CRLB generalises to the quantum case in the obvious manner. Stated together with the classical version, it says that

$$\mathrm{Var}\,\tilde{\eta} \geq \left(M I_\eta\right)^{-1} \geq \left(M J(\rho_\eta)\right)^{-1}, \tag{3.10}$$

or, that the variance of any unbiased estimator is lower bounded by the reciprocal QFI. Thus, the quantum CRLB presents the ultimate limit of the precision of any estimation task. Importantly, the quantum Cramér-Rao lower bound is achievable, but the optimal measurement may, of course, be difficult to implement for technical reasons.

4

Publications

I'm very good at integral
and differential calculus;
I know the scientific names
of beings animalculous;

Major-General Stanley in the opera
The Pirates of Penzance
by W.S. Gilbert and A. Sullivan

All of the appended papers study the use of Gaussian probe states that are allowed to interact with a noisy attenuator channel, where the transmission is unknown. The questions that motivated this research are related to the question of how much of an advantage can be gained in probing the transmission coefficient when using a quantum state over a semi-classical coherent state. In all three papers, the TMSV state is used to prepare an entangled signal-idler pair, where the signal is allowed to interact with the lossy channel while the entangled idler is ideally stored. The returns from the lossy channel are then measured together with the retained idler, with the purpose of learning something from the interactions. The material presented in this chapter is somewhat simplified and non-comprehensive, skipping the mathematical details while the full results can be found in the appended papers.

4.1 Paper I

The material in this paper was developed primarily to discuss quantum radar in regard to two experiments that had recently been put forward at the time of publication, see Refs. [31, 32] and [33][1], claiming to realise a quantum advantage in microwaves with QI-like protocols. There were some differences in the experiments with respect to the QI protocol of Tan *et al.* [18]. First, the experiments used separate heterodyne measurements of the signal and idler pairs. Secondly, the

[1]In the initial pre-print version of this paper, it was claimed that an advantage was observed. However, the published version clarifies that the advantage is *simulated* from experimental data based on the assumption of ideal photon detection.

experiments used two-mode correlated thermal noise as a classical benchmark, rather than a coherent state, something that was criticised for being non-optimal as a classical probe in Ref. [27].

The principal goal of this paper is to further the understanding of Classically Correlated Noise (CCN) as probe state, see Section 2.3.2, and its metrological properties as a radar protocol. The discussion is approached with several different tools in this paper. First, we roughly follow the analysis of Ref. [32] and compute the Pearson's correlation coefficient between the idler and return mode, based on the cross-mode terms of the covariance matrix before measurement. The Pearson's correlation coefficient is the normalised covariance between the modes. Thus, a larger amount of correlation implies that it is easier to determine whether the return mode contains a part of the transmitted signal or not. We further quantify this benefit by producing the Receiver Operating Characteristics (ROC) under the assumption that the receiver structure performs ideal heterodyne detection of both the return- and idler quadratures. As our main method for this analysis, we compute the likelihood ratio test and apply the result of Wilks's theorem to compute the asymptotic detector performance of this test. The square correlation coefficient appears as the non-centrality parameter of the chi-squared distribution, illustrating the importance of return-idler correlations in discrimination strength.

As an example of the ROC, we compute it with parameter values that could possibly be realised with microwave technology in a laboratory environment, see Fig. 4.1. For this setup, we compare the TMSV state with two versions of the CCN state, one prepared with equal number of photons in the signal and idler modes and another with many more photons in the idler. The ratio of signal photons N_S to signal and idler photons $N_S + N_I$ is parametrised by the balance parameter β, with $\beta = 0.5$ and $\beta = 0.001$ studied, respectively. As can be seen in Fig. 4.1, the TMSV state probe and the asymmetric CCN state probe with a strong idler perform equivalently given heterodyne detection of the return and idler modes. More recently [37], it was shown that it is indeed possible to retain a quantum advantage with heterodyne detection of the *return* mode, if the idler is measured homodynely, conditioned on the outcome of the heterodyne measurement.

We also give an intuition to how heterodyne detection is non-ideal, because the correlation strength *before* measurement is a factor of $\sqrt{2}$ stronger with a TMSV state probe over the best CCN state probe. This is because heterodyne detection, even ideally, imposes an increase in variance of the outcome. This extra variance is sufficient to suppress any advantage due to stronger correlations. The discrimination strength *before* detection is further analysed with the semi-asymptotic result of the Quantum Stein's Lemma, see Eq. (3.6), using the formulas for Gaussian states from Ref. [65]. The results show that the TMSV state has an unbounded advantage $\sim \ln(1 + N_S^{-1})$ over the asymmetric CCN state in terms of error exponent in the limit of vanishing probe strength, $N_S \to 0$, and infinite number of trials, $M \to \infty$. While an unbounded advantage may seem enticing, it must

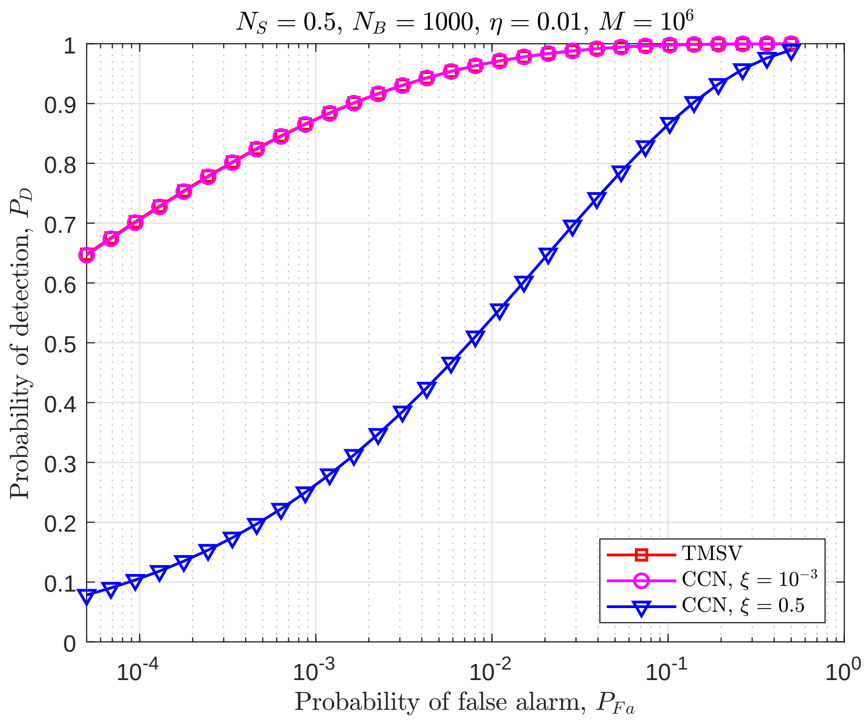

Figure 4.1: Receiver Operating Characteristic for the TMSV state probe and CCN state probe given ideal heterodyne detection of the return- and idler mode. Here, ξ refers to the balance parameter β in the text. [Reproduced from Fig. 4 of **Paper I**.]

be observed that the relative entropy tends to zero in the same limit, meaning that for $N_S = 0$ it is impossible to discriminate between the two hypotheses. The convergence to asymptotic behaviour of the error exponent is plotted in Fig. 4.2, for a finite probe strength of $N_S = 0.5$, where the TMSV state probe shows an advantage over the asymmetric CCN state probe.

Indirectly, these results also show that the asymmetric CCN state can match the performance of a coherent state probe, in the limit of a strong idler strength. That is, the classical optimality of the coherent state probe is not unique, which is interesting because the CCN state is a mixed state probe, while the TMSV and coherent state probes are pure.

Finally, since the experiments that inspired this paper used amplifiers in their setup, we analyse the impact of ideal phase-invariant amplification at various points of the protocol. While amplifying either the signal mode before transmission or the return mode at reception can be understood to impact both the TMSV and CCN probe equivalently, amplification of the idler is actually detrimental to the quantum advantage. In terms of correlations, we compute a simple criterion for when amplification of the idler suppresses any chance of a quantum advantage. For the case of minimal-noise strong idler amplification, a no-go for quantum advantage is $\beta(1-\beta)^{-1} \ll N_S$, where β is the CCN asymmetry parameter.

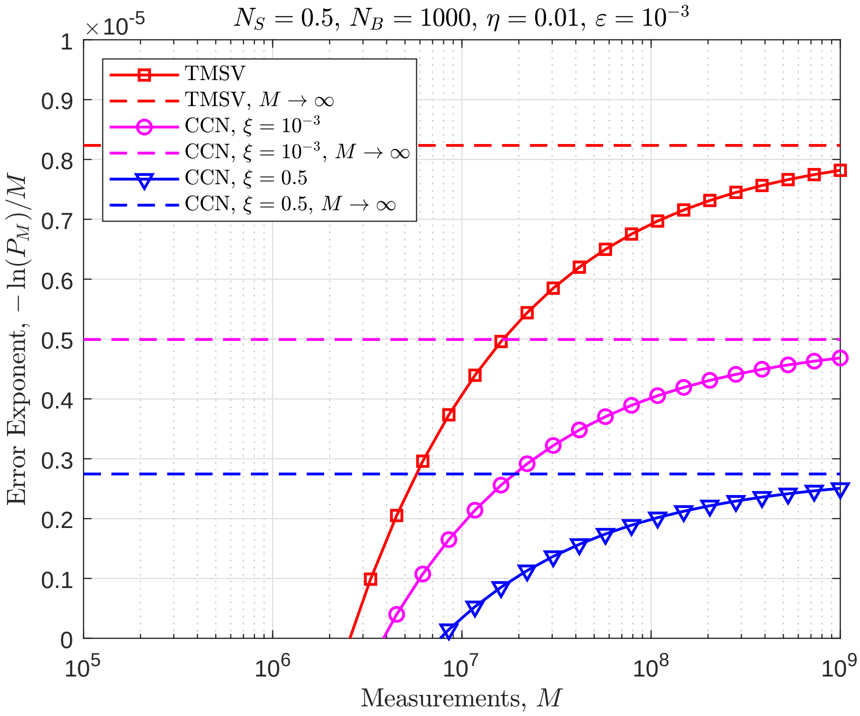

Figure 4.2: Semi-asymptotic behaviour of the error exponent with increasing number of repeated trials. The TMSV state probe outperforms the optimized CCN probe, illustrating together with Fig. 4.1 how double heterodyne measurement is non-ideal. Here, ξ refers to the balance parameter β in the text. [Reproduced from Fig. 5 of **Paper I**.]

Since the publication of **Paper I**, there has been some further study of how phase-*sensitive* amplification may still be applied in the QI protocol, see Ref. [72] but the results are, again, not in favour of any amplification. It would seem that the benefits of quantum enhanced signals like to stay in the regime where quantum effects are relevant.

4.2 Paper II

This paper was prepared for the specific purpose of bridging a perceived gap in terminology and assumptions between radar engineers and quantum optics researchers with respect to quantum radar, targeting the former as audience. For this reason, the paper is organized as two relatively separate parts, addressing in order the questions "*Without worrying about technological challenges, what is the advantage of using the quantum illumination protocol for radar?*", and "*Without worrying about the applications, what technologies are available to implement a full quantum illumination experiment?*". In some sense, this work complements that of Daum [73] where an estimate as to the cost of a working quantum radar was analysed and the main observation was that it would be considerably more expensive than conventional radar. A high cost, however, could be acceptable if sufficient benefit was offered. Our analysis in this paper actually indicates the opposite: the advantage is so situational and technically complicated that it is difficult to even imagine an operational scenario where its implementation would provide a crucial benefit.

The first of our questions is approached in a relatively straightforward manner, where the 'radar equation' is used to quantify performance. The radar equation, while it has many forms, is a tool used by radar engineers to determine, given system parameters, at what distance the radar can detect targets of a particular size. Central to the analysis is the restrictions imposed by the regime in which QI exhibits its advantage, *i.e.*, where the signal photons are few ($N_S \ll 1$) and the background is bright ($N_B \gg 1$). Inherently, this is a setting where discrimination is difficult for any device, because the receiver has to find a signal of size $\sim \eta N_S$ against noise of size N_B. That is, the SNR per mode is proportional to $\frac{\eta N_S}{N_B} \ll 1$. To compensate for this low SNR and achieve an acceptable performance of discrimination, a large number of independent trials M must be performed, and this number scales directly with the time-bandwidth product of coherent integration. In other words, a wide-band signal must be integrated for a long time for the inherently low SNR per mode to be useful. In this paper we assume, quite generously, that $M = 10^9$ may be achievable with a microwave system, given a bandwidth of 1 GHz and integration time of 1 s. Even larger time-bandwidth products would start to approach unfeasibility for moving targets. With a strong background of $N_B = 1000$, which approximately holds true for room-temperature thermal radiation in the microwave regime, this time-bandwidth product would allow for $\eta N_S \sim 10^{-5}$ if the integrated SNR is required to exceed a threshold of

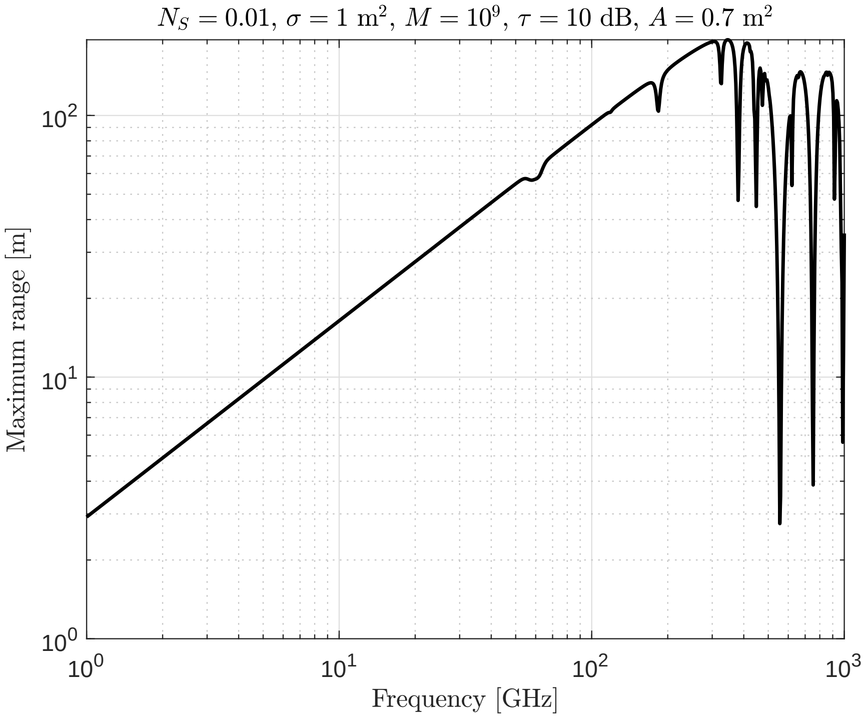

Figure 4.3: Example of maximum operating range of a quantum enhanced radar system with a fixed antenna size footprint of $A = 0.7$ m^2, a detection threshold of $\tau = 10$ and a target RCS of $\sigma = 1$ m^2. The benefit of operating at higher frequencies is explained by larger antenna directivity. The losses at frequencies larger than 300 GHz are due to significant atmospheric attenuation. [Reproduced from Fig. 1 of **Paper II**]

$\tau = 10$ before a detection is declared. For a typical radar scenario, operating at tens of kilometres, the transmit-to-receive ratio of power easily falls in the range of 10^{-15}, and may even be smaller than that. Thus, by restricting the system to operate in the regime with a quantum advantage, with $N_S < 1$, there is a discrepancy of at least ten orders of magnitude in η between what is technically realistic and what is required to approach the performance of conventional radar. We illustrated this simple calculation with the metric of maximum operating range, see Fig. 4.3, showing that, if a quantum radar is built to operate in a regime where it shows any advantage over a coherent state, it is limited to tens of metres even if all technological challenges are disregarded.

To answer the second question of technical realisability of a microwave quantum radar experiment, we look at the state-of-the-art research in the fields of entanglement sources and photon-resolving detectors at different frequency bands. We purposefully do not include infrared and visible light technologies in this study, because the ambient background is non-bright and quantum advantage scenario would be hinging on the existence of jamming. While there are promising technological candidates in the frequency ranges of tens to hundreds of gigahertz, we rule them out in favour of the more well developed microwave regime – with superconductive elements based on Josephson junction technology – for quantum illumination-like experiments.

4.3 Paper III

In this paper, we move from the quantum illumination task of channel discrimination to the task of quantum *estimation*. That is, instead of trying to determine if the transmission is zero or finite, the task is to estimate the value of the transmission coefficient. We restrict the space of probe states to the Gaussian states, expanding on previous work on the topic [74–76]. The thermal lossy Bosonic channel has the property that, for these input states, the output will also be Gaussian. Computing QFI for generic states can be complicated, and one may be have to resort to numerics. Luckily, computing the QFI is relatively accessible analytically for Gaussian states. Our tool of this study is the QFI and the quantum CLRB, in the sense that we investigate which input state, restricted to a certain power, maximises the QFI of the channel transmission. A maximum QFI implies that the estimator variance can be minimised.

Our work in this paper consists of a full characterisation of the optimal Gaussian probe state per mode, when the probes are single-mode or two-mode, with a signal and signal-idler pair, respectively. We consider also the case when these probes are repeatedly used for M independent measurements, as illustrated in Fig. 3.2, and study the *total* energy-constrained QFI. Even though this is a single-parameter estimation problem, there are several degrees of freedom in the generic Gaussian state, and the optimal state depends on the value of the three scenario parameters, meaning the average number of signal photons N_S, the average number of thermal background photons N_B and the true value of the transmission η. It may seem counter-intuitive to establish an optimal probe state for measuring an unknown η if that state depends explicitly on the value of η. One may resolve this by considering adaptive strategies, where the estimate and probe state are refined with repeated measurements, in an iterative procedure.

Crucial for this analysis to be approachable and to establish analytical results was to find canonical forms of the probe states with few degrees of freedom. The most significant simplification is simply the observation that the optimal probe state can be taken as a pure state, reducing the number of free parameters. Further reductions to the parameter space is achieved by finding symmetries in the Bosonic channel, and in simplifications of the resulting QFI, done with computer algebra software.

First, when the analysis is restricted to single-mode states with no ancillary idler mode, we show that the canonical form of the probe state has only one free parameter that describes the trade-off between local squeezing and displacement, if the total number of photons is kept fixed. The final scalar optimisation was done with exhaustive search. See Fig. 4.4 for the optimal amount of squeezing

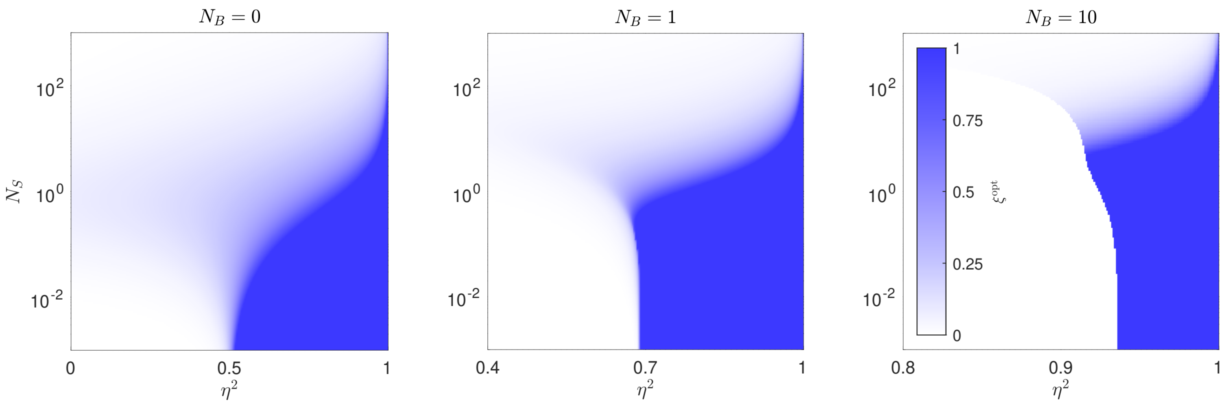

Figure 4.4: Optimal trade-off of between squeezing ($\xi = 1$) and displacement ($\xi = 0$) for the single-mode QFI for three different average numbers of background photons. For finite background ($N_B > 0$) and few probe photons ($N_S \lesssim 1$), a sharp transition between coherent state and squeezed vacuum being the optimal state is observed at low signal brightness. [Reproduced from Fig. 2 of **Paper III**.]

with vacuum ($N_B = 0$), moderate ($N_B = 1$) and strong ($N_B = 10$) background.

Interestingly, in the vacuum background where $N_B = 0$, we have that, for *any* finite η, the optimal state is a displaced squeezed state, indicating that squeezing is always resourceful. In fact, the optimised single-mode QFI grows without bound in the limit of $\eta \to 1$, showing a $(1-\eta^2)^{-1}$-divergent advantage over the classical coherent state probe, which has a QFI of $4N_S$. Away from this limit the optimal state is generally a non-trivial trade-off between squeezing and displacement, with finite squeezing for all $\eta > 0$.

When the analysis is extended to optimising the total energy-constrained QFI $\mathcal{J}_\eta = MJ(\rho_\eta)$, we study the case where we fix the total number of photons $\mathcal{N}_S = MN_S$ and optimise the probe state also over the number of modes. We establish that, in the vacuum case, the optimal allocation is either to use one single mode with all energy $M = 1$, or to use as many modes as possible, equally distributing the available energy over all modes, depending on the scenario. The boundary between these extremes has the overall structure that is similar to Fig. 4.4, see Fig. 6 in **Paper III**.

Outside of the vacuum case, we find that the probe that maximises the total QFI always uses the maximum number of available modes. This is because of the ‘shadow effect’ that gives the receiver information about η based on the background photons alone, independently of the probe.

We do also briefly study the variant of the channel where the number of background photons is normalised to be independent of the transmission coefficient, known as the “no passive signature assumption” [7]. We show that, in this setting, the optimal state is the infinite number of trials ($M \to \infty$) TMSV probe state with vanishing photons per mode. We prove this result by computing the QFI for this state and showing that it actually saturates the fundamental upper bound proved in Ref. [61]. The result that TMSV is universally optimal when the shadow effect is removed was first reported without proof at the 2021 International Symposium on Information Theory [77]. After our publication of **Paper III**, a longer version of Ref. [77] was published as Ref. [78].

5

Conclusion and Outlook

In short, in matters vegetable,
animal, and mineral;
I am the very model
of a modern Major-Gineral;

Major-General Stanley in the opera
The Pirates of Penzance
by W.S. Gilbert and A. Sullivan

The material covered in this thesis is based on a project that has been mainly concerned with the metrological power of quantum Gaussian states with focus on quantum radar. We have studied both the setting of symmetric and asymmetric binary discrimination, mimicking the scenario of radar-like operation. To complement this, we have also comprehensively studied the task of estimating the loss parameter with generic Gaussian states and established results of optimality. These types of problems illustrate some fascinating features of nature at the quantum scale, and it is no surprise that there is that hope significant technological benefits are possible by the exploitation of these features. Nevertheless, we have found that metrological quantum advantages can be elusive when one tries to apply them to practical tasks.

In our work with the appended publications, we strived to maintain a high level of mathematical rigour and correctness in the material with regard to the quantum description, while still making the material available to readers with different theoretical backgrounds. Importantly, our two conference papers target primarily an audience more familiar with radar technology and signal processing, rather than the experts on quantum metrology.

For the particular case of quantum radar in terms of the quantum illumination protocol, we claim that it fails to be useful for conventional radar operation. There are several fundamental reasons for this conclusion even when the technological challenge itself is disregarded. We need to discuss these reasons in some detail to understand why we would discard the quantum radar concept. For one, if the quantum illumination advantage is to be realised, the quantum enhanced setup has to be compared to a conventional radar operating with a coherent state with few average photons – essentially only slightly different from the vacuum state. Comparing this type of setup with one of a conventional radar operating with signals in power range of kilowatts can simply not be considered fair, since using a signal that can be 20 orders of magnitude stronger trivially outperforms a system using only a few photons. We emphasize that increasing the number of photons in the quantum enhanced state probe does in no way fail the protocol. Indeed, as can be understood intuitively, a stronger signal will be able to perform the discrimination task better. The crux of the matter is that a strong quantum enhanced signal will be no better than a coherent state probe operating with a signal consisting of the same number of photons. Thus, without other constraints there is no reason not to use as strong a coherent state probe as possible, since it's preparation is comparatively simple, and the performance is optimal. Next, there have been proposals to prepare the quantum state with few photons per mode, and then increase the signal strength to useful levels with amplification. Our analysis have shown, both with general arguments and analytical results, that an amplified quantum enhanced signal will, again, not perform any better than a coherent state operating at that power level.

Does this mean that quantum illumination is not useful? the answer of course depends on what is required for something to be useful. The scheme itself is highly relevant as an example in the ongoing work to push the limits of metrology, and it maintains its peculiar feature that entanglement appears resourceful, even though the lossy channel breaks entanglement before measurement. Thus, the protocol itself is highly relevant for this field of physics. Outside of the strictly theoretical interest of the relation between quantum advantage and entanglement, quantum illumination and variants of the protocol may still find practical applications to certain tasks with sensitive samples, where it is beneficial to use as weak a signal as possible. For example, there may be other binary tests, such as quantum reading or imaging, that can be enhanced with such a probe. Our shift from discrimination to quantum estimation in **Paper III** was made with the purpose of broadening the scope of the project and increase the knowledge of other aspects of quantum metrology.

Looking forward, this broader scope can hopefully be maintained. An interesting question is whether there are other quantum enhanced benefits of extending the analyses of these problems to non-Gaussian probe states. As we have shown, Gaussian probes can be shown to be ideal for some problems, and in these cases there is definitely no further advantage to be found with a larger set of possible states. However, there may be situations where extending the analysis to consider also classes of non-Gaussian probe states allows for finding further quantum advantages, or advantages in other regimes. An interesting challenge with this extension would be in the loss of the possibility of analytical calculations, as one often has to resort to numerical techniques in computing, for example, the quantum Fisher information for non-Gaussian states. Another topic that has seen research efforts lately is the study of simpler receiver structures that allow for the implementation of quantum enhanced protocols such as quantum illumination and it will be interesting to follow the experimental development of those technologies.

A

Appendix

A.1 Computing Gaussian Quantum Fisher Information

In this section, we show how the computation of the quantum Fisher information of an unknown parameter θ can be computed for a Gaussian state with mean vector $\vec{d}_\theta$ and covariance matrix $\mathbf{\Sigma}_\theta$. Since the density operators of Gaussian states live in infinite dimensional Hilbert spaces, direct computation is not applicable. Following the book by Serafini [51], we make an *Ansatz* that, for the Gaussian states, the SLD is at most quadratic in the quadrature operators $\hat{r} = (\hat{q}_1, \hat{p}_1, \ldots, \hat{q}_n, \hat{p}_n)^\top$. That is, we assume the SLD takes the form

$$\hat{\mathcal{L}} = L_0 + \vec{L}_1^\top \hat{r} + \hat{r}^\top \mathbf{L}_2 \hat{r}, \tag{A.1}$$

where L_0 is a scalar, $\vec{L}_1$ is a vector, and $\mathbf{L}_2$ is a quadratic form. By application of some further relations, the Gaussian quantum Fisher information can be computed as

$$J(\rho_\theta) = \mathrm{tr}\left[\mathbf{L}_2 \left(\partial_\theta \mathbf{\Sigma}_\theta\right)\right] + (\partial_\theta \vec{d}_\theta)^\top \mathbf{\Sigma}_\theta^{-1} (\partial_\theta \vec{d}_\theta), \tag{A.2}$$

where the quadratic form $\mathbf{L}_2$ is determined by the equation

$$2\partial_\theta \mathbf{\Sigma} = 4\mathbf{\Sigma}\mathbf{L}_2\mathbf{\Sigma} + \mathbf{\Omega}\mathbf{L}_2\mathbf{\Omega}. \tag{A.3}$$

For the single- and two-mode states studied here, the covariance matrix is at most of size 4×4 such that Eq. (A.3) can be solved by *vectorization*, where solving the 16×16 system of equations

$$\left(4\mathbf{\Sigma}^\top \otimes \mathbf{\Sigma} + \mathbf{\Omega}^\top \otimes \mathbf{\Omega}\right) \mathrm{vec}\left(\mathbf{L}_2\right) = 2\,\mathrm{vec}\left(\partial_\theta \mathbf{\Sigma}\right), \tag{A.4}$$

is equivalent [79].

Let $\mathbf{M} \in \mathbb{R}^{M \times N}$ be a matrix. Vectorization is the map 'vec' transforming the

$M \times N$ matrix to the $MN \times 1$ vector by stacking the matrix columns. That is, for

$$\mathbf{M} = \begin{pmatrix} m_{1,1} & m_{1,2} & \dots & m_{1,N} \\ m_{2,1} & m_{2,2} & \ddots & \vdots \\ \vdots & \ddots & \ddots & \vdots \\ m_{M,1} & \dots & \dots & m_{M,N} \end{pmatrix} \tag{A.5}$$

the vectorization is

$$\text{vec}\left(\mathbf{M}\right) = \begin{pmatrix} m_{1,1} & m_{2,1} & \dots & m_{M,1} & m_{1,2} & \dots & m_{M,N} \end{pmatrix}^\top . \tag{A.6}$$

An important identity, referred to as *Roth's Relationship* [80], is $\text{vec}(\mathbf{ABC}) = (\mathbf{C}^\top \otimes \mathbf{A})\,\text{vec}\left(\mathbf{B}\right)$. This allows us to solve the equation $\mathbf{AXA} + \mathbf{BXB} = \mathbf{C}$ for $\mathbf{X}$ by inverting the matrix $\mathbf{A}^\top \otimes \mathbf{A} + \mathbf{B}^\top \otimes \mathbf{B}$.

Bibliography

[1] G. Galati. *100 Years of Radar*. 1st ed. Springer International Publishing Switzerland, 2016. ISBN: 978-3-319-00583-6. DOI: 10.1007/978-3-319-00584-3.

[2] D. S. Ilcev. "The development of maritime radar. Part 1: Before the Second World War". In: *International Journal of Maritime History* 32.4 (2020), pp. 996–1007. DOI: 10.1177/0843871420977963.

[3] J. D. Jackson. *Classical Electrodynamics*. 1st ed. John Wiley & Sons, 1999. ISBN: 978-0-471-30932-1.

[4] C. W. Helstrom. "Quantum detection and estimation theory". In: *Journal of Statistical Physics* 1 (1969), pp. 231–252.

[5] J. Aasi et al. "Enhanced sensitivity of the LIGO gravitational wave detector by using squeezed states of light". In: *Nature Photonics* 7.8 (2013), pp. 613–619. DOI: 10.1038/nphoton.2013.177.

[6] L. McCuller et al. "Frequency-Dependent Squeezing for Advanced LIGO". In: *Phys. Rev. Lett.* 124 (2020), p. 171102. DOI: 10.1103/PhysRevLett.124.171102.

[7] S. Pirandola et al. "Advances in photonic quantum sensing". In: *Nature Photonics* 12 (2018), pp. 724–733. DOI: 10.1038/s41566-018-0301-6.

[8] M. Lanzagorta. *Quantum Radar*. Springer Nature Switzerland AG 2022, 2011. ISBN: 978-3-031-02515-0. DOI: 10.1007/978-3-031-02515-0.

[9] R. G. Torromé, N. B. Bekhti-Winkel, and P. Knott. "Introduction to quantum radar". In: *arXiv:2006.14238 [quant.ph]* (2021). DOI: 10.48550/arXiv.2006.14238.

[10] G. Sorelli et al. "Detecting a Target With Quantum Entanglement". In: *IEEE Aerospace and Electronic Systems Magazine* 37.5 (2022), pp. 68–90. DOI: 10.1109/MAES.2021.3116323.

[11] E. H. Allen and M. Karageorgis. "Radar systems and methods using entangled quantum particles". U.S. pat. 7375802B2. L. Martin. May 2008.

[12] S. Guha and Z. Dutton. "Systems and methods for quantum receivers for target detection using a quantum optical radar". U.S. pat. 8339581B2. R. B. T. Corp. Dec. 2012.

[13] G. Burdge et al. *Quantum Sensors Program.* Tech. rep. AFRL-RI-RS-TR-2009-208. 2009. URL: https://apps.dtic.mil/sti/pdfs/ADA506209.pdf (Accessed Mar. 24, 2023).

[14] S. Lloyd. "Enhanced Sensitivity of Photodetection via Quantum Illumination". In: *Science* 321.5895 (2008), pp. 1463–1465. DOI: 10.1126/science.1160627.

[15] M. F. Sacchi. "Optimal discrimination of quantum operations". In: *Phys. Rev. A* 71 (2005), p. 062340. DOI: 10.1103/PhysRevA.71.062340.

[16] M. F. Sacchi. "Entanglement can enhance the distinguishability of entanglement-breaking channels". In: *Phys. Rev. A* 72 (2005), p. 014305. DOI: 10.1103/PhysRevA.72.014305.

[17] J. H. Shapiro and S. Lloyd. "Quantum illumination versus coherent-state target detection". In: *New Journal of Physics* 11.6 (2009), p. 063045.

[18] S.-H. Tan et al. "Quantum Illumination with Gaussian States". In: *Phys. Rev. Lett.* 101 (2008), p. 253601. DOI: 10.1103/PhysRevLett.101.253601.

[19] L. Maccone and C. Ren. "Quantum Radar". In: *Phys. Rev. Lett.* 124 (2020), p. 200503. DOI: 10.1103/PhysRevLett.124.200503.

[20] S. Guha and B. I. Erkmen. "Gaussian-state quantum-illumination receivers for target detection". In: *Phys. Rev. A* 80 (2009), p. 052310. DOI: 10.1103/PhysRevA.80.052310.

[21] Q. Zhuang, Z. Zhang, and J. H. Shapiro. "Optimum Mixed-State Discrimination for Noisy Entanglement-Enhanced Sensing". In: *Phys. Rev. Lett.* 118 (2017), p. 040801. DOI: 10.1103/PhysRevLett.118.040801.

[22] R. Nair. "Discriminating quantum-optical beam-splitter channels with number-diagonal signal states: Applications to quantum reading and target detection". In: *Phys. Rev. A* 84 (2011), p. 032312. DOI: 10.1103/PhysRevA.84.032312.

[23] S. Barzanjeh et al. "Microwave Quantum Illumination". In: *Phys. Rev. Lett.* 114 (2015), p. 080503. DOI: 10.1103/PhysRevLett.114.080503.

[24] J. Hewitt. *Quantum radar can detect what's invisible to regular radar.* 2015. URL: https://www.extremetech.com/extreme/200161-quantum-radar-can-detect-whats-invisible-to-regular-radar (Accessed Dec. 10, 2022).

[25] J. Lin and P. Singer. *China Says It Has Quantum Radar: What Does That Mean?* 2016. URL: https://www.popsci.com/china-says-it-has-quantum-radar-what-does-that-mean/ (Accessed Dec. 10, 2022).

[26] E. D. Lopaeva et al. "Experimental Realization of Quantum Illumination". In: *Phys. Rev. Lett.* 110 (2013), p. 153603. DOI: 10.1103/PhysRevLett.110.153603.

[27] J. H. Shapiro. "The Quantum Illumination Story". In: *IEEE Aerospace and Electronic Systems Magazine* 35.4 (2020), pp. 8–20. DOI: 10.1109/MAES.2019.2957870.

[28] Z. Zhang et al. "Entanglement-Enhanced Sensing in a Lossy and Noisy Environment". In: *Phys. Rev. Lett.* 114 (2015), p. 110506. DOI: 10.1103/PhysRevLett.114.110506.

[29] D. G. England, B. Balaji, and B. J. Sussman. "Quantum-enhanced standoff detection using correlated photon pairs". In: *Phys. Rev. A* 99 (2019), p. 023828. DOI: 10.1103/PhysRevA.99.023828.

[30] P. S. Blakey et al. "Quantum and non-local effects offer over 40 dB noise resilience advantage towards quantum lidar". In: *Nature Communications* 13 (2022), p. 5633. DOI: 10.1038/s41467-022-33376-9.

[31] C. W. S. Chang et al. "Quantum-enhanced noise radar". In: *Applied Physics Letters* 114.11 (2019), p. 112601. DOI: 10.1063/1.5085002.

[32] D. Luong et al. "Receiver Operating Characteristics for a Prototype Quantum Two-Mode Squeezing Radar". In: *IEEE Transactions on Aerospace and Electronic Systems* 56.3 (2020), pp. 2041–2060. DOI: 10.1109/TAES.2019.2951213.

[33] S. Barzanjeh et al. "Microwave quantum illumination using a digital receiver". In: *Science Advances* 6.19 (2020). DOI: 10.1126/sciadv.abb0451.

[34] E. T. from the arXiv. *Quantum radar has been demonstrated for the first time.* 2019. URL: https://www.technologyreview.com/2019/08/23/75512/quantum-radar-has-been-demonstrated-for-the-first-time/ (Accessed Mar. 23, 2023).

[35] R. Assouly et al. "Demonstration of Quantum Advantage in Microwave Quantum Radar". In: (2022). DOI: 10.48550/ARXIV.2211.05684.

[36] J. Angeletti et al. "Microwave quantum illumination with correlation-to-displacement conversion". In: *arXiv:2303.18206 [quant-ph]* (2023). DOI: 10.48550/arXiv.2303.18206.

[37] H. Shi, B. Zhang, and Q. Zhuang. "Fulfilling entanglement's optimal advantage via converting correlation to coherence". In: *arXiv: 2207.06609 [quant-ph]* (2022). DOI: 10.48550/arXiv.2207.06609.

[38] M. Reichert et al. "Quantum Illumination with a Hetero-Homodyne Receiver and Sequential Detection". In: *arXiv:2303.18207 [quant-ph]* (2023). DOI: 10.48550/arXiv.2303.18207.

[39] K. Durak, N. Jam, and Ç. Dindar. "Object tracking and identification by quantum radar". In: *Quantum Technologies and Quantum Information Science V*. Ed. by M. T. Gruneisen et al. Vol. 11167. International Society for Optics and Photonics. SPIE, 2019. DOI: 10.1117/12.2550479.

[40] Q. Zhuang and J. H. Shapiro. "Ultimate Accuracy Limit of Quantum Pulse-Compression Ranging". In: *Phys. Rev. Lett.* 128 (2022), p. 010501. DOI: 10.1103/PhysRevLett.128.010501.

[41] M. Reichert et al. "Quantum-enhanced Doppler lidar". In: *npj Quantum Information* 8 (2022). DOI: 10.1038/s41534-022-00662-9.

[42] U. Las Heras et al. "Quantum illumination reveals phase-shift inducing cloaking". In: *Scientific Reports* 7 (2017). DOI: 10.1038/s41598-017-08505-w.

[43] Q. Zhuang, Z. Zhang, and J. H. Shapiro. "Quantum illumination for enhanced detection of Rayleigh-fading targets". In: *Phys. Rev. A* 96 (2017), p. 020302. DOI: 10.1103/PhysRevA.96.020302.

[44] E. Jung and D. Park. "Quantum illumination with three-mode Gaussian state". In: *Quantum Information Processing* 21 (2022), p. 71. DOI: 10.1007/s11128-021-03359-8.

[45] R. Loudon. *The Quantum Theory of Light*. 3rd ed. Oxford University Press, 2000. ISBN: 978-0-19-850176-3.

[46] S. Barnett and P. Radmore. *Methods in Theoretical Quantum Optics*. 1st ed. Oxford University Press, 1997. ISBN: 0-19-856362-0.

[47] C. Cohen-Tannoudji, J. Dupont-Roc, and G. Grynberg. *Photons and Atoms. Introduction to Quantum Electrodynamics*. 1st ed. John Wiley & Sons, Inc., 1989. ISBN: 0-471-18433-0.

[48] H. Goldstein, C. Poole, and J. Safko. *Classical Mechanics*. 3rd ed. Pearson Education Limited, 2002. ISBN: 978-1-292-02655-8.

[49] C. Weedbrook et al. "Gaussian quantum information". In: *Rev. Mod. Phys.* 84 (2012), pp. 621–669. DOI: 10.1103/RevModPhys.84.621.

[50] G. Adesso, S. Ragy, and A. R. Lee. "Continuous variable quantum information: Gaussian states and beyond". In: *Open Systems and Information Dynamics* 21.1 & 2 (2014), p. 1440001. DOI: 10.1142/S1230161214400010.

[51] A. Serafini. *Quantum continuous variables: a primer of theoretical methods*. 1st ed. CRC press, 2017. ISBN: 978-1-4822-4634-6.

[52] J. H. Shapiro. "The Quantum Theory of Optical Communications". In: *IEEE Journal of Selected Topics in Quantum Electronics* 15.6 (2009), pp. 1547–1569. DOI: 10.1109/JSTQE.2009.2024959.

[53] S. H. Tan. "Quantum state discrimination with bosonic channels and Gaussian states". Massachusetts Institute of Technology. PhD thesis. 2010. URL: http://hdl.handle.net/1721.1/79253 (Accessed Nov. 12, 2022).

[54] C. M. Caves. "Quantum limits on noise in linear amplifiers". In: *Physical Review D* 26.8 (1982), pp. 1817–1839. DOI: 10.1103/PhysRevD.26.1817.

[55] D. Braun et al. "Quantum-enhanced measurements without entanglement". In: *Rev. Mod. Phys.* 90 (2018), p. 035006. DOI: 10.1103/RevModPhys.90.035006.

[56] S. M. Kay. *Fundamentals of Statistical Signal Processing: Detection Theory*. Prentice-Hall, Inc., 1998. ISBN: 0-13-504135-X.

[57] S. S. Wilks. "The Large-Sample Distribution of the Likelihood Ratio for Testing Composite Hypotheses". In: *The Annals of Mathematical Statistics* 9.1 (1938), pp. 60–62. ISSN: 00034851. URL: http://www.jstor.org/stable/2957648 (Accessed Apr. 3, 2023).

[58] K. M. R. Audenaert et al. "Discriminating States: The Quantum Chernoff Bound". In: *Phys. Rev. Lett.* 98 (2007), p. 160501. DOI: 10.1103/PhysRevLett.98.160501.

[59] S. Pirandola and S. Lloyd. “Computable bounds for the discrimination of Gaussian states”. In: *Phys. Rev. A* 78 (2008), p. 012331. DOI: 10.1103/PhysRevA.78.012331.

[60] T. Kailath. “The Divergence and Bhattacharyya Distance Measures in Signal Selection”. In: *IEEE Transactions on Communication Technology* 15.1 (1967), pp. 52–60. DOI: 10.1109/TCOM.1967.1089532.

[61] R. Nair and M. Gu. “Fundamental limits of quantum illumination”. In: *Optica* 7.7 (2020), pp. 771–774. DOI: 10.1364/OPTICA.391335.

[62] J. Calsamiglia et al. “Local discrimination of mixed states”. In: *Physical review letters* 105.8 (2010), p. 080504. DOI: 10.1103/PhysRevLett.105.080504.

[63] A. Karsa and S. Pirandola. “Classical benchmarking for microwave quantum illumination”. In: *IET Quantum Communication* 2.4 (2021), pp. 246–257. DOI: https://doi.org/10.1049/qtc2.12025.

[64] C. Weedbrook et al. “How discord underlies the noise resilience of quantum illumination”. In: *New Journal of Physics* 18.4 (2016), p. 043027. DOI: 10.1088/1367-2630/18/4/043027.

[65] M. M. Wilde et al. “Gaussian Hypothesis Testing and Quantum Illumination”. In: *Phys. Rev. Lett.* 119 (2017), p. 120501. DOI: 10.1103/PhysRevLett.119.120501.

[66] Q. Zhuang, Z. Zhang, and J. H. Shapiro. “Entanglement-enhanced Neyman-Pearson target detection using quantum illumination”. In: *J. Opt. Soc. Am. B* 34 (2017), pp. 1567–1572. DOI: 10.1364/JOSAB.34.001567.

[67] F. Hiai and D. Petz. “The proper formula for relative entropy and its asymptotics in quantum probability”. In: *Communications in mathematical physics* 143 (1991), pp. 99–114. DOI: 10.1007/BF02100287.

[68] T. Ogawa and H. Nagaoka. “Strong converse and Stein’s lemma in quantum hypothesis testing”. In: *IEEE Transactions on Information Theory* 46.7 (2000), pp. 2428–2433. DOI: 10.1109/18.887855.

[69] G. De Palma and J. Borregaard. “Minimum error probability of quantum illumination”. In: *Phys. Rev. A* 98 (2018), p. 012101. DOI: 10.1103/PhysRevA.98.012101.

[70] K. Li. “Second-order asymptotics for quantum hypothesis testing”. In: *The Annals of Statistics* 42.1 (2014), pp. 171–189. DOI: 10.1214/13-AOS1185.

[71] S. M. Kay. *Fundamentals of Statistical Signal Processing: Estimation Theory.* Prentice-Hall, Inc., 1993. ISBN: 0-13-345711-7.

[72] J. N. Blakely. “Quantum-Correlated Noise Radar with Phase-Sensitive Amplification”. In: *2021 IEEE Radar Conference (RadarConf21).* 2021, pp. 1–6. DOI: 10.1109/RadarConf2147009.2021.9455243.

[73] F. Daum. “Quantum radar cost and practical issues”. In: *IEEE Aerospace and Electronic Systems Magazine* 53 (2020), pp. 8–20. DOI: 10.1109/MAES.2020.2982755.

[74] A. Monras and M. G. A. Paris. "Optimal Quantum Estimation of Loss in Bosonic Channels". In: *Phys. Rev. Lett.* 98 (2007), p. 160401. DOI: 10.1103/PhysRevLett.98.160401.

[75] A. Monras and F. Illuminati. "Measurement of damping and temperature: Precision bounds in Gaussian dissipative channels". In: *Phys. Rev. A* 83 (2011), p. 012315. DOI: 10.1103/PhysRevA.83.012315.

[76] R. Nair. "Quantum-Limited Loss Sensing: Multiparameter Estimation and Bures Distance between Loss Channels". In: *Phys. Rev. Lett.* 121 (2018), p. 230801. DOI: 10.1103/PhysRevLett.121.230801.

[77] Z. Gong et al. "Fundamental Limits of Loss Sensing over Bosonic Channels". In: *2021 IEEE International Symposium on Information Theory (ISIT)*. 2021, pp. 1182–1187. DOI: 10.1109/ISIT45174.2021.9517810.

[78] Z. Gong et al. "Quantum-Enhanced Transmittance Sensing". In: *IEEE Journal of Selected Topics in Signal Processing* (2022), pp. 1–17. DOI: 10.1109/JSTSP.2022.3222680.

[79] A. J. Laub. *Matrix analysis for scientists and engineers.* 1st ed. Society for Industrial and Applied Mathematics, 2005. ISBN: 0-89871-576-8.

[80] H. D. Macedo and J. N. Oliveira. "Typing linear algebra: A biproduct-oriented approach". In: *Science of Computer Programming* 78.11 (2013), pp. 2160–2191. DOI: 10.1016/j.scico.2012.07.012.